Report

www.the-innovation.org

Revolution of vitamin E production by starting from microbial fermented farnesene to isophytol

Ziling Ye,[1,2] Bin Shi,[1,2] Yanglei Huang,[1] Tian Ma,[1] Zilei Xiang,[1] Ben Hu,[1] Zhaolin Kuang,[1] Man Huang,[2] Xiaoying Lin,[1] Zhu Tian,[1] Zixin Deng,[1] Kun Shen,[1] and Tiangang Liu[1,*]

*Correspondence: liutg@whu.edu.cn

Received: December 18, 2021; Accepted: March 8, 2022; Published Online: March 12, 2022; https://doi.org/10.1016/j.xinn.2022.100228

GRAPHICAL ABSTRACT

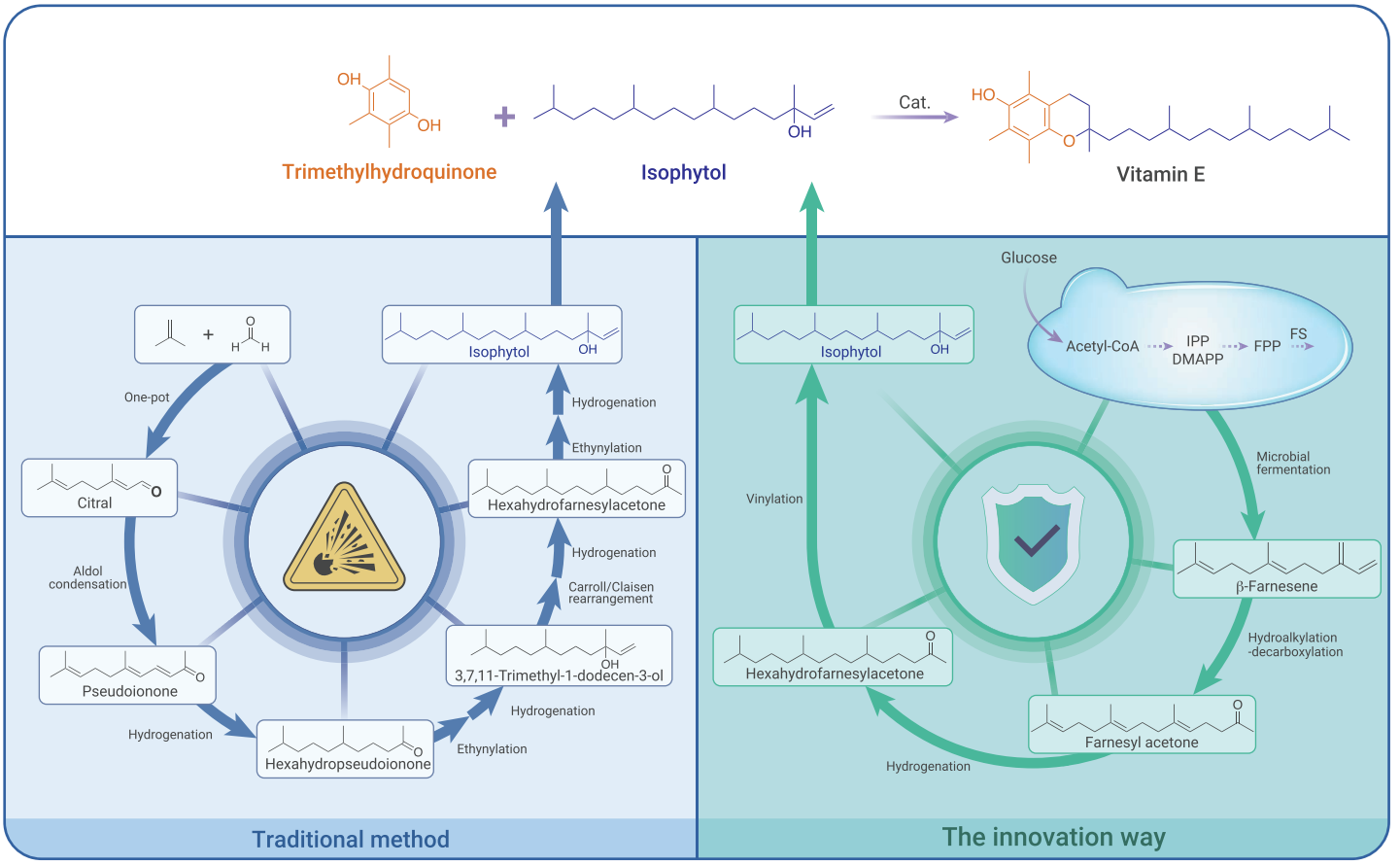

PUBLIC SUMMARY

- The traditional chemical synthesis of vitamin E is complex and could be explosive
- An innovative way to synthesize isophytol from biofermented farnesene is established
- This process is safer and cheaper, changing the production and marketing of vitamin E
- Co-production of β-farnesene and lycopene improves the competitiveness of this process

Report

Revolution of vitamin E production by starting from microbial fermented farnesene to isophytol

Ziling Ye,[1,2] Bin Shi,[1,2] Yanglei Huang,[1] Tian Ma,[1] Zilei Xiang,[1] Ben Hu,[1] Zhaolin Kuang,[1] Man Huang,[2] Xiaoying Lin,[1] Zhu Tian,[1] Zixin Deng,[1] Kun Shen,[1] and Tiangang Liu[1,*]

[1]Key Laboratory of Combinatorial Biosynthesis and Drug Discovery, Ministry of Education and School of Pharmaceutical Sciences, Wuhan University, Wuhan 430071, China
[2]J1 Biotech Co., Ltd., Wuhan 430075, China
*Correspondence: liutg@whu.edu.cn

Received: December 18, 2021; Accepted: March 8, 2022; Published Online: March 12, 2022; https://doi.org/10.1016/j.xinn.2022.100228

Citation: Ye Z., Shi B., Huang Y., et al., (2022). Revolution of vitamin E production by starting from microbial fermented farnesene to isophytol. The Innovation **3(3)**, 100228.

Vitamin E is one of the most widely used vitamins. In the classical commercial synthesis of vitamin E (α-tocopherol), the chemical synthesis of isophytol is the key technical barrier. Here, we establish a new process for isophytol synthesis from microbial fermented farnesene. To achieve an efficient pathway for farnesene production, *Saccharomyces cerevisiae* was selected as the host strain. First, β-farnesene synthase genes from different sources were screened, and through protein engineering and system metabolic engineering, a high production of β-farnesene in *S. cerevisiae* was achieved (55.4 g/L). This farnesene can be chemically converted into isophytol in three steps with approximately 92% yield, which is economically equal to that from the best total chemical synthesis. Furthermore, we co-produced lycopene and farnesene to reduce the cost of farnesene. A factory based on this new process was successfully operated in Hubei Province, China, in 2017, with an annual output of 30,000 tons of vitamin E. This new process has completely changed the vitamin E market due to its low cost and safety.

INTRODUCTION

Vitamin E is the general term for tocopherols and tocotrienols, essential fat-soluble vitamins for humans.[1] It has a wide range of physiological functions based on its antioxidation properties, including improving the body's immunity and fertility, possessing anti-cancer and anti-inflammatory properties, heart protection, nerve protection, and other functional characteristics.[2-4] Thus, it is widely used in feed additives, medicine, food, cosmetics, and other fields. Together with vitamins C and A, it is listed as one of the three pillar products of the vitamin series.

Vitamin E includes natural and synthetic vitamin E. For industrial production, natural vitamin E is mainly extracted from vegetable oil deodorizer distillate and other plants rich in vitamin E.[5] Although this process preserves its natural activity, the low yield, complex extraction and purification processes, and dependence on the climate and culture make it difficult to meet the market demand. Only 20% of vitamin E comes from plant extraction.[6] With the development of biotechnology, the biosynthetic pathway of vitamin E has been elucidated.[7,8] In plants, vitamin E biosynthesis is initiated by homogentisate synthesized by the shikimate pathway and various hydrophobic polyprenyl pyrophosphates that determine the final type of vitamin E. Geranylgeranyl pyrophosphate (GGPP) derived from the 2C-methyl-D-erythritol-4-phosphate pathway is the precursor for tocotrienol, and phytyl pyrophosphate obtained from GGPP reduction or chlorophyll degradation followed by phosphorylation is used for tocopherol biosynthesis (Figure 1A).[9,10] Researchers have attempted to increase the vitamin E content of plants by pathway engineering. Overexpression of barley homogentisate geranylgeranyl transferase, which catalyzes the committed step of tocotrienol biosynthesis in *Arabidopsis thaliana* leaves, resulted in a 10- to 15-fold increase in tocotrienol and tocopherol levels,[7] and its overexpression in soybean seeds has also sufficiently increased tocochromanol levels by 8- to 10-fold.[11] In *Nicotiana benthamiana*, the transient expression of tocopherol cyclase and homogentisate phytyltransferase from *A. thaliana* has increased α-tocopherol levels by 11.3 fold.[12] However, it is still difficult to meet the increasing market demand for vitamin E.

Currently, 80% of commercial vitamin E comes from chemical synthesis, and it is mainly consumed in the feed industry. Classical synthesis of vitamin E (α-tocopherol) is via the condensation of isophytol and trimethylhydroquinone, and the production capacity and cost largely depend on the production of these two materials. Due to the increasing demand for vitamin E, many different synthetic routes have been developed and optimized to synthesize vitamin E precursors. The *M*-cresol and pseudoionone processes are the main synthetic routes for synthesizing trimethylhydroquinone and isophytol,[13] respectively. By 2017, the classical processes used to synthesize isophytol and trimethylhydroquinone were relatively mature, and the entire market price of vitamin E was approximately US$20/kg based on the use of classical technology.

The rapid development of metabolic engineering and synthetic biology has made the microbial cell factory a game changer in chemical production.[14] The efficient production of various compounds, such as the anti-cancer drug taxol precursor taxadiene,[15] anti-malarial drug precursor artemisinic acid,[16,17] advanced biofuel short-chain alkanes,[18] fatty acids,[19,20] and biopolymer polyhydroxyalkanoates,[21] has demonstrated the advantages and potential of microbial fermentation in terms of cost effectiveness. Some studies have also achieved the heterologous synthesis of vitamin E in microorganisms. Albermann et al. heterologously expressed vitamin E biosynthesis genes from *Synechocystis* and *A. thaliana* in *Escherichia coli*, resulting in 15 μg/g δ-tocotrienols.[22] The *de novo* production of δ-tocotrienol from glucose with a titer of 4.1 mg/L in fed-batch fermentation was achieved in *S. cerevisiae*.[23] Furthermore, Shen et al. comprehensively optimized the vitamin E heterologous pathway and the endogenous precursor pathway, designed a cold-shock-triggered temperature control system, and successfully constructed high-tocotrienol-producing *S. cerevisiae* with the production of 320 mg/L.[24] Although these studies have laid the foundation for the production of vitamin E by microbial fermentation, continued efforts are warranted to ensure the possibility of commercial production.

In 2014, our group efficiently synthesized farnesene by refactoring the mevalonate (MVA) pathway in *E. coli*.[25] In the same year, Nenter & Co. innovated the synthesis of trimethylhydroquinone and was eagerly looking for a way to break through the isophytol synthesis process.[26] Upon noticing this need, we proposed a new innovative process of using biofermented farnesene as a substrate to synthesize isophytol to subvert the isophytol synthesis pathway (Figure 1C). Here, we provide a retrospect on how this disruptive new approach was established in detail.

RESULTS

Evaluating the possibility of different methods to generate isophytol

We evaluated potential routes for synthesizing vitamin E based on cost, safety, and efficiency. Previously, vitamin E could be obtained only by plant extraction and chemical synthesis. Chemical synthesis of vitamin E has great advantages and occupies the entire market in the feedstock industry. It is achieved by condensing isophytol and trimethylhydroquinone (Figure 1D). The synthesis of trimethylhydroquinone is relatively easy, whereas the chemical synthesis of isophytol is difficult. The pseudoionone process is the classical process used to prepare isophytol and is initiated by the condensation of citral and acetone to pseudoionone,[27] and isophytol can be obtained by hydrogenation, ethynylation, and condensation of pseudoionone in seven steps (Figure 1B).[28] This process involves a multistep alkyne reaction under high pressure, with high requirements for equipment and safety.

Synthetic biology is a highly safe procedure used to produce bulk chemicals with a low environmental burden. However, several difficulties are associated with the microbial synthesis of vitamin E by heterologous expression of synthetic genes from plants or other suitable resources. First, this biosynthesis pathway needs to introduce multiple heterologous genes with many uncertainties regarding their protein expression and catalytic efficiency. Meanwhile, achieving a high titer of intracellular products with the relatively higher molecular weights and cell toxicity is difficult.[29-32] Most importantly, the cost of the chemical synthesis of vitamin E is approximately US$10/kg; thus, it is

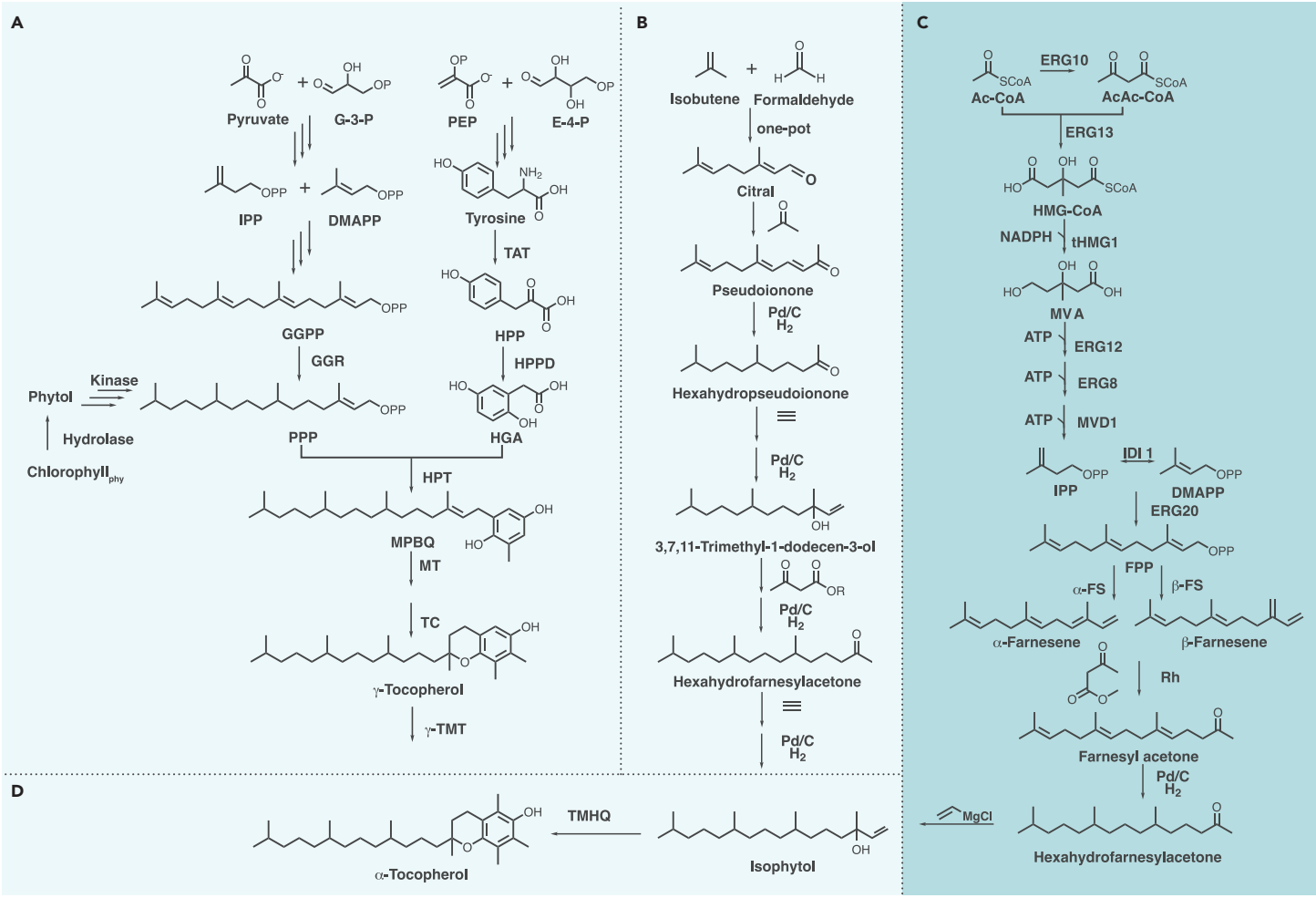

Figure 1. Synthesis of vitamin E (A) Vitamin E biosynthetic pathway in plants. G-3-P, D-glyceraldehyde 3-phosphate; IPP, isopentenyl diphosphate; DMAPP, dimethylallyl diphosphate; GGPP, geranylgeranyl pyrophosphate; PPP, phytyl diphosphate; PEP, phosphoenolpyruvate; E-4-P, D-erythrose 4-phosphate; HPP, 4-hydroxyphenylpyruvate; HGA, homogentisic acid; MPBQ, 2-methyl-6-phytylquinol; GGR, geranylgeranyl reductase; HPPD, 4-hydroxyphenylpyruvate dioxygenase; HPT, homogentisate phytyltransferase; MT, 2-methyl-6-phytylbenzoquinol methyltransferase; TC, tocopherol cyclase; γ-TMT, γ-tocopherol methyltransferase. (B) Traditional synthesis process of isophytol. (C) Farnesene biosynthetic pathway in *S. cerevisiae* and new process for isophytol synthesis discussed in this study. Ac-CoA, acetyl-CoA; AcAc-CoA, acetoacetyl-CoA; HMG-CoA, (S)-3-hydroxy-3-methylglutaryl-CoA; MVA, (R)-mevalonate; MVP, (R)-5-phosphomevalonate; MVPP, (R)-5-diphosphomevalonate; FPP, farnesyl diphosphate; ERG10, acetoacetyl-CoA thiolase; ERG13, hydroxymethylglutaryl-CoA synthase; tHMG1, truncated 3-hydroxy-3-methylglutaryl-CoA reductase; ERG12, mevalonate kinase; ERG8, phosphomevalonate kinase; MVD1, mevalonate-5-pyrophosphate decarboxylase; IDI1, isopentenylpyrophosphate isomerase; ERG20, farnesyl pyrophosphate synthase; α-FS, α-farnesene synthase; β-FS, β-farnesene synthase. (D) Chemical synthesis of vitamin E. TMHQ, trimethylhydroquinone.

difficult for a process using fermented vitamin E to compete with this in a short period.

Isophytol is the key chemical intermediate for vitamin E chemical synthesis, and phytol obtained by chlorophyll degradation can also be used as a precursor for vitamin E synthesis.[33,34] However, there are few studies on isophytol biosynthesis by microorganisms and phytol synthesis. Furthermore, phytol and isophytol are long-carbon-chain alcohols, and in previous studies, other long-carbon-chain alcohols, such as fatty alcohols, were found to be highly toxic; their accumulation in cells would affect the growth of strains and eventually lead to low yields.[35-37] Therefore, we considered that replacing the existing isophytol chemical synthesis process with the microbial synthesis of phytol/isophytol would not be an optimal choice.

In 2014, our group constructed a farnesene-overproducing strain by engineering key enzymes in *E. coli* based on the information obtained from *in vitro* reconstitution.[25] Farnesene can be secreted out of the cell and has no obvious effect on the growth of the strain; furthermore, it is easy to realize highly efficient synthesis in the microorganism. For the past 10 years, most groups considered that farnesene was only the precursor for jet fuel. However, we previously conceived a process to obtain farnesyl acetone via farnesene,[38] which was then converted to isophytol by hydrogenation and addition reactions (Figure 1C). In this process, the three-step reaction via the conversion of farnesene to isophytol can simplify the synthesis process and reduce the use of explosive raw materials.

Therefore, this new method for synthesizing isophytol via farnesene obtained by microbial fermentation could be promising in producing vitamin E.

Evaluation of α- or β-farnesene to isophytol

Farnesene includes α- and β-farnesene, and discrepancies in their structures may influence the efficiency of conversion to isophytol. To validate our proposed process for the synthesis of isophytol using farnesene as a substrate, *E. coli* F4[25], with nearly 2 g/L production reported in previous work, was fermented for α-farnesene preparation; after 100 h of shake-flask fermentation, the strain was extracted with hexane/ethyl acetate (4:1) and then separated using silica gel column chromatography to obtain α-farnesene with 95% purity, as confirmed by nuclear magnetic resonance. *S. cerevisiae* T16 (CEN.PK2-1D with an additional copy of *tHMG1*, *FgJ03939*, and *ERG20*) was used for β-farnesene preparation, and the method for compound isolation was consistent with that reported previously.[39]

For the chemical synthesis of isophytol, Rh-catalyzed alkylation of farnesene with methyl acetoacetate and subsequent decarboxylation under alkaline conditions afforded farnesyl acetone **1** and **1′** (supplemental materials and methods). The yield of farnesyl acetone was only 11% using α-farnesene as the substrate, while that using β-farnesene was 95%. The difference in yields obtained using α- or β-farnesene as the substrate may be the result of different substitutions on 1,3-butadiene in α- and β-farnesene. In addition, farnesyl acetone was further converted to hexahydrofarnesylacetone (**2**) in 98% yield using the catalyst Pd/C in methanol under an H_2 atmosphere (supplemental materials and methods). The

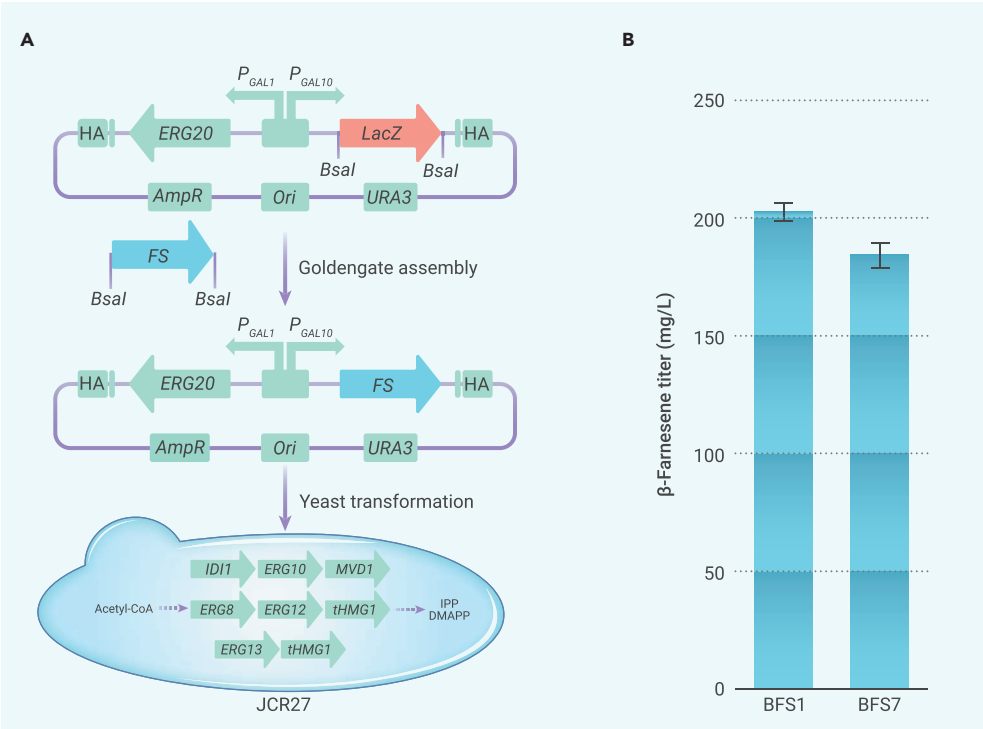

Figure 2. Screening of farnesene synthases for β-farnesene production in *S. cerevisiae* (A) Flowchart of plasmid and strain construction for gene screening. *ERG20*, farnesyl pyrophosphate synthase from *S. cerevisiae*; *ERG10*, acetyl-CoA acetyltransferase from *S. cerevisiae*; *ERG13*, 3-hydroxy-3-methylglutaryl CoA synthase from *S. cerevisiae*; *tHMG1*, truncated 3-hydroxy-3-methylglutaryl CoA reductase from *S. cerevisiae*; *ERG12*, mevalonate kinase from *S. cerevisiae*; *ERG8*, phosphomevalonate kinase from *S. cerevisiae*; *MVD1*, mevalonate diphosphate decarboxylase from *S. cerevisiae*; and *IDI1*, isopentenyl diphosphate isomerase from *S. cerevisiae*. (B) β-farnesene production by strains with β-farnesene synthase from different sources. BFS1 contains β-farnesene synthase of *M. chamomilla* var. *recutita* and BFS7 contains β-farnesene synthase of *A. annua*. Error bars indicate the standard deviations of three biological replicates.

reaction was performed at room temperature and atmospheric pressure hydrogen without heating and high pressure; it was safe and energy efficient. Isophytol (**3**) was obtained in 99% yield by the reaction of hexahydrofarnesylacetone (**2**) with vinyl magnesium chloride in tetrahydrofuran under an N_2 atmosphere (supplemental materials and methods).

This three-step reaction can be used to realize the conversion of β-farnesene obtained by microbial fermentation to isophytol, with an overall yield of 92%. This result demonstrates the excellent potential of this new process to replace the traditional process of isophytol synthesis. In 2017, the process from farnesene to isophytol and further to vitamin E verified in this study was successfully put into production by Nenter & Co. in Jingzhou, Hubei Province, China, and an annual output of 30,000 tons of vitamin E has since been achieved.

Efficient microbial synthesis of farnesene

The conversion of farnesene to isophytol was confirmed. However, whether this process is revolutionary depends on the yield, titer, and productivity of farnesene. Therefore, the efficient synthesis of farnesene is very important, and in this study, we aimed to achieve high production of β-farnesene.

Chassis selection. *E. coli* is easily infected by phages; it is not very good for biomass use and is not tolerant to high farnesene concentrations. Compared with *E. coli*, *S. cerevisiae* is generally regarded as safe and robust under harsh industrial conditions,[40] and it was thus selected as the chassis strain. Farnesyl diphosphate (FPP) is derived from the MVA pathway for sesquiterpene synthesis, and the weak synthetic capacity of the native MVA pathway in yeast limits the production of sesquiterpenes.[41,42] To achieve high production, the flux of the MVA pathway needs to be increased.[43] We used the CRISPR-Cas9 system for MVA pathway engineering to avoid a lack of markers. First, the *Cas9* gene from the type II bacterial CRISPR system of *Streptococcus pyogenes* was integrated into CEN.PK 2-1D to generate JCR1. Then *ERG8*, *tHMG1* (two copies) and *ERG12*, *MVD1*, *ERG10*, *IDI1*, and *ERG13* under the control of P_{GAL1}-P_{GAL10} and P_{GAL7} were overexpressed in the JCR1 genome via three integration steps to generate JCR27. Our group successfully produced sesquiterpene guaia-6,10(14)-diene at a high titer in a previous study based on this precursor-providing platform;[44] therefore, strain JCR27, with overexpression all the MVA pathway genes, was used as the platform strain.

Selection of farnesene synthase. Farnesene is present in various plants and varies in content. For gene screening, we selected *Mac-bFS* from *Matricaria chamomilla* var. *recutita* (GenBank: AIG92847.1)[45] and *Aa-bFS* from *Artemisia annua* (GenBank: AAX39387.1),[46] both of which have been isolated and characterized. To expand the screening ranges for β-farnesene synthases, we also selected several putative β-farnesene synthases from the NCBI database, including predicted β-farnesene synthases from *Helianthus annuus* (GenBank: KAF5755268), *Tanacetum cinerariifolium* (GenBank: GEU62861.1), *Cynara cardunculus* (GenBank: XP_024994934.1), and *Lactuca sativa* (GenBank: XP_023749309.1). *ERG20* to improve FPP flux and β-farnesene synthase under the control of P_{GAL1}-P_{GAL10} were overexpressed by episomal plasmids in the MVA-overexpressing strain JCR27, resulting in strains BFS1 (*Mac-bFS*), BFS2 (*Hea-bFS*), BFS4 (*Tac-bFS*), BFS5 (*Cyc-bFS*), BFS6 (*Las-bFS*), and BFS7 (*Aa-bFS*). BFS1 produced 203 ± 3.8 mg/L β-farnesene after 72 h of incubation, which was higher than that produced by BFS7 (184 ± 5.27 mg/L) (Figure 2B), but strains BFS2, 4, 5, and 6 failed to detect the target product *in vivo*, indicating that the activity of β-farnesene synthase from *M. chamomilla* var. *recutita* was higher in *S. cerevisiae* than that of others. Therefore, *Mac-bFS* was chosen for use in the next construction.

Farnesene synthase engineering. The catalytic efficiency of farnesene synthase determines the flux from FPP to farnesene. Further enhancing the catalytic activity of farnesene synthase can increase the titer of farnesene. Directed evolution is a powerful strategy used to change the catalytic activity of enzymes, and it is possible to obtain mutants with improved performance based on a suitable targeted screening method.[47,48] In this study, directed evolution was employed to improve the *Mac-bFS* activity. The crystal structure of farnesene synthase from *M. chamomilla* var. *recutita* has not been solved yet; therefore, a random approach was adopted to mutate *Mac-bFS* (Figure 3). To isolate improved farnesene synthase variants, we developed a simple high-throughput screening method to single out improved farnesene synthase variants that detect the content difference of farnesene in strains based on the vanillin-sulfuric acid method. The expression of wild-type farnesene synthases resulted in low absorbance, and mutants with improved farnesene synthase activity were identified based on their higher absorbance. We screened β-farnesene synthase mutants from a library of about 2,000 transformants, and mutants with an increased β-farnesene yield were selected. After further shake-flask fermentation, plasmid extraction, and sequencing, we identified mutations in pBFS9 (F11S, TTC-TCC), pBFS12 (M35T, ATG-ACC), pBFS15 (T319S, ACT-TCT), pBFS18 (I434T, ATT-ACT), and pBFS20 (I460V, ATC-GTC), and the production in these variants was 1.46-, 1.23-, 1.12-, 1.40-, and 1.21-fold, respectively, compared with that in BFS1 with wild-type β-farnesene synthase (Table S1).

The 3D structure of proteins, including those in BFS1 (wild type), BFS9 (F11S), BFS12 (M35T), BFS15 (T319S), BFS18 (I434T), and BFS20 (I460V), was simulated using SWISS-MODEL (https://swissmodel.expasy.org/), and the crystal structure of (+)-delta-cadinene synthase (PDB: 3G4D) was used as the template for wild-type and mutant modeling. The substrate FPP was docked to the simulated structures using AutoDock 4, and the binding site for the docking procedure was defined according to the crystal structure of another homologous sesquiterpene synthase (PDB: 4RNQ). The docking parameters were set as default. The results showed that the distance between the five mutation sites and FPP was more than 5 Å. The docking results are shown in Figures S1–S6. In addition,

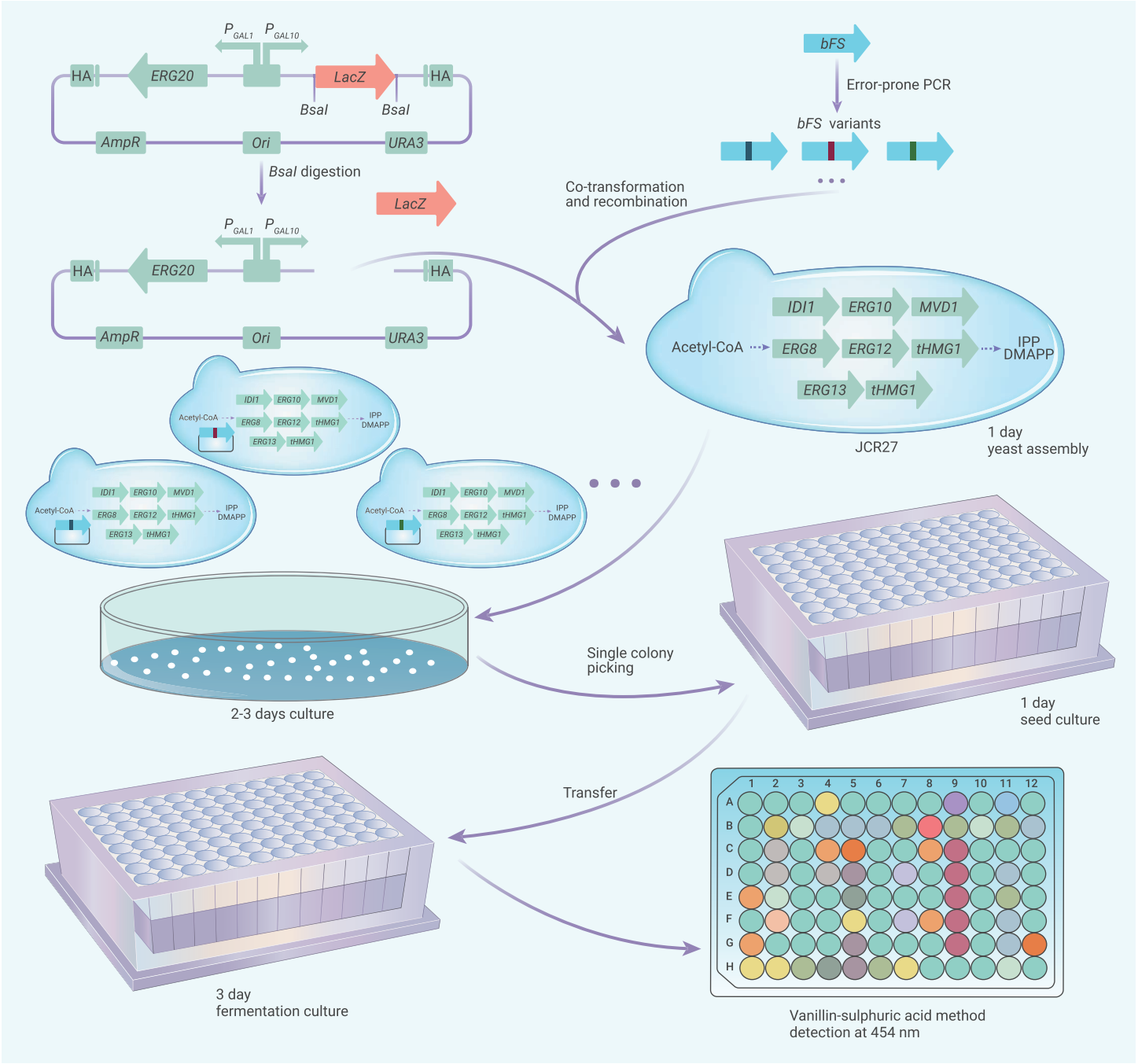

Figure 3. Overview of screening procedures for β-farnesene synthase variants

the docking binding energy between FPP and the enzymes showed that the five mutations had a stronger affinity with the substrate than the wild type (Table S1); therefore, we inferred that this might be the reason for the increase in activity. The beneficial effects of single mutations are often additive;[49] therefore, we combined the improved mutation in *Mac-bFS*, and the best β-farnesene synthase variant BFS45 (F11S, M35T, T319S, I434T, I460V) improved the titer by approximately 2-fold.

Pathway engineering. The expression system of chromosomal integration is preferred over an episomal plasmid for industrial applications as it is more stable.[50] Therefore, for the construction of producing strains, all modifications to the host strain were made by chromosomal integration. pBFS45 harboring the FPP synthase Erg20 and the best β-farnesene synthase variant was linearized and integrated into the JCR27 genome, and JVA122 was obtained with a β-farnesene titer of 437 mg/L (Figure 4).

To achieve commercially viable farnesene production, metabolic fluxes must be fine-tuned to maximize farnesene titers. The farnesene biosynthetic pathway can be divided into an upstream MVA pathway and a downstream farnesene synthetic pathway. We adopted a "push-pull" strategy to balance the upstream and downstream fluxes and tuned the copy number of the rate-limiting enzyme tHMG1 in the upstream pathway and farnesene synthase in the downstream pathway to increase the production. β-farnesene production increased with the increase in copy number, and the titer in the β-farnesene-producing strain JVA139 with a copy number of 5 for Mac-bFS45 based on JCR27 was 791 mg/L (Figure 4). We further deleted *GAL80* to constitutively express all heterologous genes under the control of galactose-inducible promoters, and the titer of the resulting strain JVA140 reached up to 736 mg/L, without the addition of galactose, which would thus reduce the fermentation cost.

Farnesene overproduction by high-cell-density fermentation

To test the performance of JVA140 for farnesene production, we conducted fed-batch fermentation in 1 L bioreactors. The fermentation media are listed in the supplemental materials and methods. Under two-stage

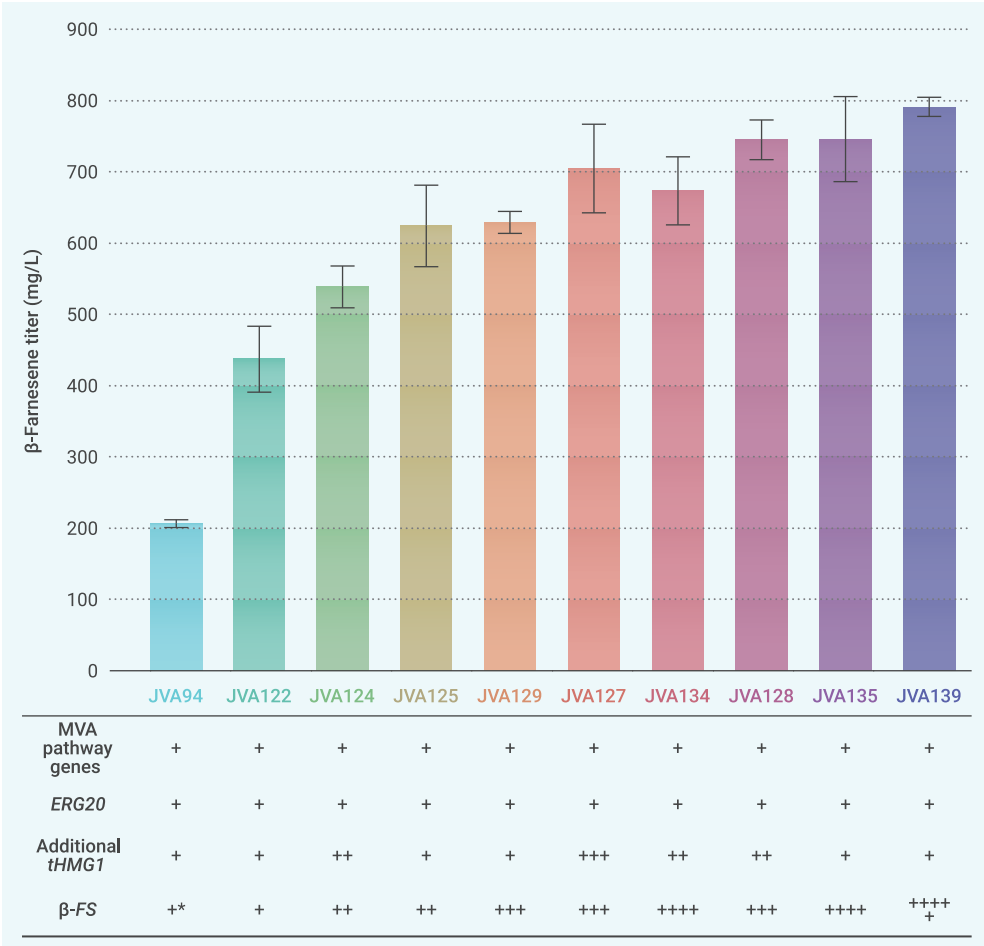

Figure 4. β-farnesene production by fine-tuning *FS* and *tHMG1* Effects of the expression of different copy numbers of *Mac-bFS* (F11S, M35T, T319S, I434T, I460V) and *tHMG1* on β-farnesene production in *S. cerevisiae*. +* means wild-type β-farnesene *Mac-bFS*. Error bars indicate the standard deviations of three biological replicates.

fermentation, biomass accumulated quickly in the first stage, and the products accumulated after glucose exhaustion. At the beginning of fermentation, the glucose concentration was 40 g/L; it was then consumed due to cell growth, and when it was close to 1 g/L, feeding solution I was added at a controlled feeding rate to sustain cell growth and to maintain the glucose concentration at approximately 0–1 g/L. Furthermore, 10% v/v isopropyl myristate was added to cultures at 24 h to reduce product loss. When cell growth slowed, feeding solution II was used for product accumulation, and the ethanol concentration was maintained at 5–10 g/L. JVA140 achieved a titer of 55.4 g/L β-farnesene and a yield of 6.5% grams of farnesene per gram of glucose after 126 h cultivation (Figure 5A).

The new process of vitamin E synthesis using farnesene was considered to have a competitive cost advantage over that of chemical vitamin E synthesis only when the microbial fermentation cost for farnesene was estimated to be lower than US$6/kg. However, the carbon cost of JVA140 microbial fermentation for farnesene is approximately US$6/kg. As the titer by Amyris can reach 130 g/L of β-farnesene and the glucose conversion rate of nearly 20% in yeast, with a carbon cost of US$2.3/kg, which was the minimum cost calculated based on the price of glucose (US$0.4/kg),[51] Nenter & Co. further collaborated with Amyris to provide β-farnesene as the raw material for vitamin E synthesis using this new process; however, it is generally necessary to further reduce the fermentation cost to improve the competitiveness.

Co-production of farnesene and lycopene

We envisaged the introduction of high-value-added compounds based on farnesene-producing strains to reduce the microbial synthesis cost. Lycopene is an excellent antioxidant with favorable physiological effects and is widely used in the health care product market; the demand and market for lycopene have increased dramatically. Our group has previously conducted a considerable amount of research on the microbial synthesis of lycopene,[29-31,52] and we have a relatively solid experimental foundation; therefore, we considered introducing the lycopene synthesis pathway into the farnesene-producing strain. In a previous study, the optimal combination of *PaCrtE* from *Pantoea ananatis*, *PagCrtB* from *P. agglomerans*, and *BtCrtI* from *B. trispora* was obtained, and *tHMG1*, *CrtE*, and *CrtI* were found to be the rate-limiting enzymes in the lycopene biosynthesis pathway.[30] For lycopene overproduction in the farnesene-producing strain, ribosomal DNA multi-copy integration of *PaCrtE*, *BtCrtI*, and *PagCrtB*, *tHMG1* was implemented in JVA139 to obtain mutants. Red colonies were selected to integrate *URA3* and delete *GAL80* to generate a prototrophic and non-galactose-inducible strain. JZL32 can produce 106 ± 6 mg/L β-farnesene and 63 ± 5 mg/L lycopene after 72 h incubation. It was evident that the farnesene titer was reduced significantly with lycopene production, mainly because of the competition for the common precursor FPP. JZL32 was subjected to 1 L fed-batch fermentation, and the β-farnesene and lycopene titers reached 616 and 419 mg/L (6.5 mg/g dry cell weight (DCW)), respectively, at 120 h (Figure 5B). The overall yield was 0.16% grams of products per gram of glucose, with a carbon cost of approximately US$600/kg lycopene plus 1.5 kg β-farnesene; although the cost is still high, the market price of lycopene is nearly US$2,000/kg, which can cover the fermentation cost. Therefore, microbial fermentation for farnesene accompanied by lycopene is almost a cost-free process, and only the purification cost needs to be considered.

DISCUSSION

Vitamin E is one of the most in-demand vitamin products in the global market. At present, the global annual demand is approximately 80,000 tons. The price of vitamin E fluctuates with the price of raw materials. In this study, we proposed a new process for synthesizing the vitamin E precursor isophytol. The process uses biosynthetic farnesene as the substrate to synthesize isophytol prior to synthesizing vitamin E. We first converted farnesene to isophytol, and the three-step reaction can realize a traditional seven-step process. The new process is efficient, is safe, and uses fewer explosive raw materials. Based on this new process proposed and verified in this study, a plant with 30,000 ton capacity per year was established in Jingzhou, Hubei Province, through the efforts of Nenter & Co. (200 km from Wuhan University) and has been in production since 2017. The process used is conducive for stabilizing the supply and price of vitamin E. As such, the market price of vitamin E has dropped from US$20/kg to approximately US$10/kg. This process combines synthetic biology with chemical synthesis, and the production safety of this process is greatly improved compared with that of previous methods. In addition, carbon dioxide emissions are reduced by 50%. The process is thus illustrative of the success of using synthetic biology to improve the classical chemical process.

Currently, 20% of the global vitamin E yield is produced using this process, and Nenter & Co. uses β-farnesene provided by the factory of Amyris in Brazil due to the company's lower-cost fermented β-farnesene. Further improving the titer and yield of the microbial fermentation of farnesene would make this process more competitive. We developed our method by first achieving the overproduction of β-farnesene in *S. cerevisiae* through systematic metabolic engineering; however, the titer and yield were not sufficient for the method to replace the use of chemical synthesis. The lycopene synthesis pathway was then introduced into the high-production strain of farnesene, and this realized the "cost-0" synthesis of

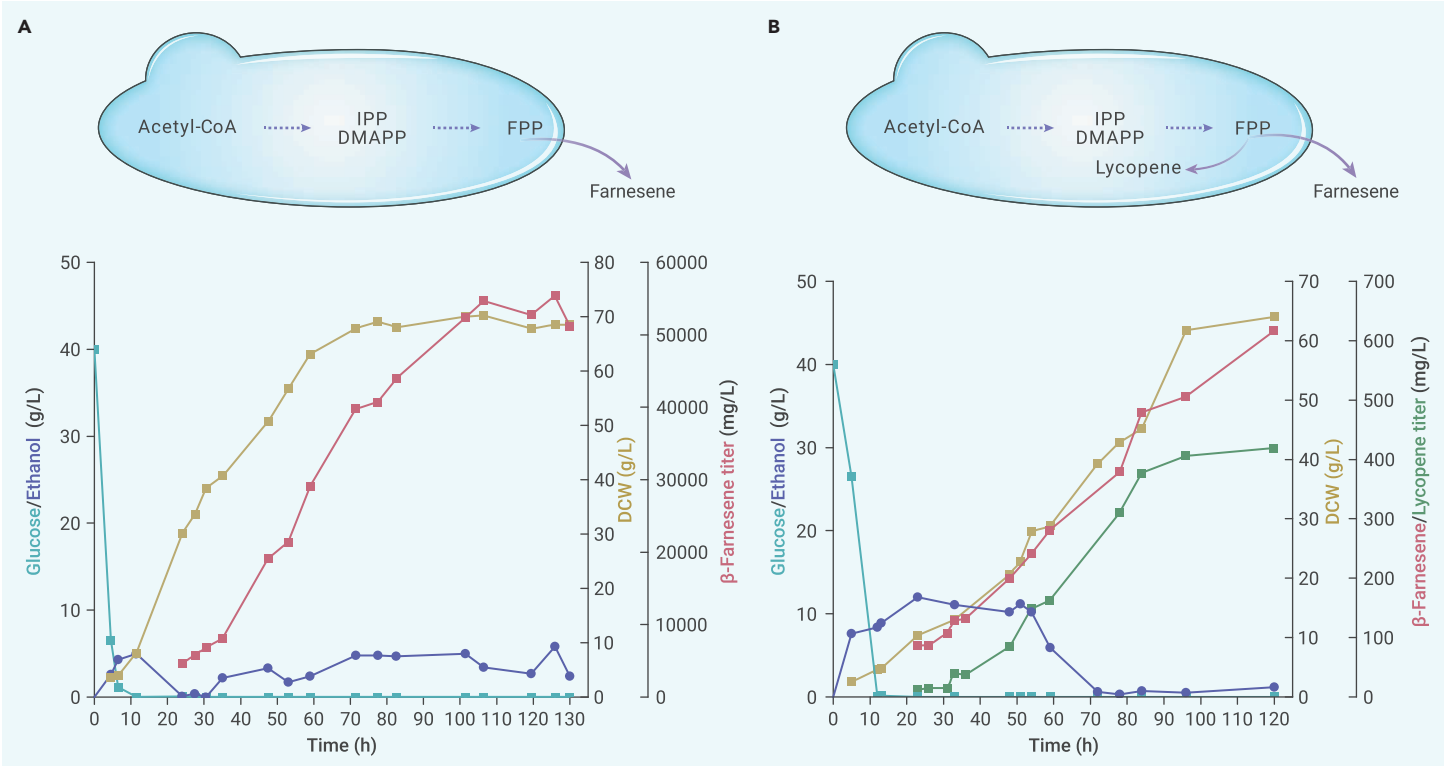

Figure 5. β-farnesene and lycopene production in bioreactors (A) Fed-batch fermentation of JVA140 in a 1 L bioreactor. (B) Fed-batch fermentation of JZL32 in a 1 L bioreactor.

farnesene accompanied by the production of the high-value-added antioxidant lycopene by microbial fermentation. However, there was a significant reduction in the production of farnesene when producing it together with lycopene due to precursor competition, which may increase the difficulty of extraction. In the future, we can further optimize the microbial fermentation pathway and reduce the synthetic cost of farnesene in two ways: (1) by rewriting the central carbon metabolism to improve precursor supply, downregulating the competitive pathway, and prolonging the period of high productivity by introducing a genetic circuit that can be used to improve the titer and yield of farnesene and (2) by improving the microbial fermentation process of farnesene production by using products in the non-MVA pathway, such as inositol and succinic acid, which may be promising to reduce costs. It is anticipated that with further advances, the remaining 80% of the vitamin E capacity may be replaced by this process in the future.

REFERENCES

1. Peh, H.Y., Tan, W.S., Liao, W., and Wong, W.S. (2016). Vitamin E therapy beyond cancer: tocopherol versus tocotrienol. Pharmacol. Ther. ***162***, 152–169.
2. Lee, G.Y., and Han, S.N. (2018). The role of vitamin E in immunity. Nutrients ***10***, 1614.
3. Mohd Mutalip, S.S., Ab-Rahim, S., and Rajikin, M.H. (2018). Vitamin E as an antioxidant in female reproductive health. Antioxidants ***7***, 22.
4. Alqahtani, S., and Kaddoumi, A. (2015). Vitamin E transporters in cancer therapy. AAPS J. ***17***, 313–322.
5. Li, M., Pham, P.J., Pittman, C.U., et al. (2008). Selective solid-phase extraction of alpha-tocopherol by functionalized ionic liquid-modified mesoporous SBA-15 adsorbent. Anal. Sci. ***24***, 1245–1250.
6. Ogbonna, J.C. (2009). Microbiological production of tocopherols: current state and prospects. Appl. Microbiol. Biotechnol. ***84***, 217–225.
7. Cahoon, E.B., Hall, S.E., Ripp, K.G., et al. (2003). Metabolic redesign of vitamin E biosynthesis in plants for tocotrienol production and increased antioxidant content. Nat. Biotechnol. ***21***, 1082–1087.
8. Zeng, Z., Han, N., Liu, C., et al. (2020). Functional dissection of *HGGT* and *HPT* in barley vitamin E biosynthesis via CRISPR/Cas9-enabled genome editing. Ann. Bot. ***126***, 929–942.
9. Mene-Saffrane, L. (2017). Vitamin E biosynthesis and its regulation in plants. Antioxidants ***7***, 2.
10. Muñoz, P., and Munné-Bosch, S. (2019). Vitamin E in plants: biosynthesis, transport, and function. Trends Plant Sci. ***24***, 1040–1051.
11. Konda, A.R., Nazarenus, T.J., Nguyen, H., et al. (2020). Metabolic engineering of soybean seeds for enhanced vitamin E tocochromanol content and effects on oil antioxidant properties in polyunsaturated fatty acid-rich germplasm. Metab. Eng. ***57***, 63–73.
12. Sathish, S., Preethy, K.S., Venkatesh, R., and Sathishkumar, R. (2018). Rapid enhancement of α-tocopherol content in *Nicotiana benthamiana* by transient expression of *Arabidopsis thaliana* tocopherol cyclase and homogentisate phytyl transferase genes. 3 Biotech. ***8***, 485.
13. Netscher, T. (2007). Synthesis of vitamin. E. Vitam. Horm. ***76***, 155–202.
14. Ren, Y., Liu, S., Jin, G., et al. (2020). Microbial production of limonene and its derivatives: achievements and perspectives. Biotechnol. Adv. ***44***, 107628.
15. Ajikumar, P.K., Xiao, W.H., Tyo, K.E., et al. (2010). Isoprenoid pathway optimization for taxol precursor overproduction in *Escherichia coli*. Science ***330***, 70–74.
16. Ro, D.K., Paradise, E.M., Ouellet, M., et al. (2006). Production of the antimalarial drug precursor artemisinic acid in engineered yeast. Nature ***440***, 940–943.
17. Paddon, C.J., Westfall, P.J., Pitera, D.J., et al. (2013). High-level semi-synthetic production of the potent antimalarial artemisinin. Nature ***496***, 528–532.
18. Choi, Y.J., and Lee, S.Y. (2013). Microbial production of short-chain alkanes. Nature ***502***, 571–574.
19. Yu, T., Zhou, Y.J., Huang, M., et al. (2018). Reprogramming yeast metabolism from alcoholic fermentation to lipogenesis. Cell ***174***, 1549–1558, e14.
20. Kim, H.M., Chae, T.U., Choi, S.Y., et al. (2019). Engineering of an oleaginous bacterium for the production of fatty acids and fuels. Nat. Chem. Biol. ***15***, 721–729.
21. Ma, H., Zhao, Y., Huang, W., et al. (2020). Rational flux-tuning of *Halomonas bluephagenesis* for co-production of bioplastic PHB and ectoine. Nat. Commun. ***11***, 3313.
22. Albermann, C., Ghanegaonkar, S., Lemuth, K., et al. (2008). Biosynthesis of the vitamin E compound delta-tocotrienol in recombinant *Escherichia coli* cells. Chembiochem ***9***, 2524–2533.
23. Sun, H., Yang, J., Lin, X., et al. (2020). De novo high-titer production of delta-tocotrienol in recombinant *Saccharomyces cerevisiae*. J. Agric. Food Chem. ***68***, 7710–7717.
24. Shen, B., Zhou, P., Jiao, X., et al. (2020). Fermentative production of vitamin E tocotrienols in *Saccharomyces cerevisiae* under cold-shock-triggered temperature control. Nat. Commun. ***11***, 5155.
25. Zhu, F., Zhong, X., Hu, M., et al. (2014). In vitro reconstitution of mevalonate pathway and targeted engineering of farnesene overproduction in *Escherichia coli*. Biotechnol. Bioeng. ***111***, 1396–1405.
26. Ma, T., Deng, Z., and Liu, T. (2020). The past and present of vitamin E. Synth. Biol. J. ***1***, 174–186.
27. Kuśtrowski, P., Sułkowska, D., Chmielarz, L., and Dziembaj, R. (2006). Aldol condensation of citral and acetone over mesoporous catalysts obtained by thermal and chemical activation of magnesium–aluminum hydrotalcite-like precursors. Appl. Catal. A. ***302***, 317–324.
28. Aec Chim Organ Biolog (1967). Improvements in and Relating to Process of Preparing Isophytol, [P].
29. Ma, T., Shi, B., Ye, Z., et al. (2019). Lipid engineering combined with systematic metabolic engineering of *Saccharomyces cerevisiae* for high-yield production of lycopene. Metab. Eng. ***52***, 134–142.
30. Shi, B., Ma, T., Ye, Z., et al. (2019). Systematic metabolic engineering of *Saccharomyces cerevisiae* for lycopene overproduction. J. Agric. Food Chem. ***67***, 11148–11157.

31. Kang, W., Ma, T., Liu, M., et al. (2019). Modular enzyme assembly for enhanced cascade biocatalysis and metabolic flux. Nat. Commun. ***10***, 4248.
32. Li, L., Liu, Z., Jiang, H., and Mao, X. (2020). Biotechnological production of lycopene by microorganisms. Appl. Microbiol. Biotechnol. ***104***, 10307–10324.
33. Gutbrod, K., Romer, J., and Dörmann, P. (2019). Phytol metabolism in plants. Prog. Lipid Res. ***74***, 1–17.
34. Hunter, S.C., and Cahoon, E.B. (2007). Enhancing vitamin E in oilseeds: unraveling tocopherol and tocotrienol biosynthesis. Lipids ***42***, 97–108.
35. Liu, R., Zhu, F., Lu, L., et al. (2014). Metabolic engineering of fatty acyl-ACP reductase-dependent pathway to improve fatty alcohol production in *Escherichia coli*. Metab. Eng. ***22***, 10–21.
36. Wenning, L., Yu, T., David, F., et al. (2017). Establishing very long-chain fatty alcohol and wax ester biosynthesis in *Saccharomyces cerevisiae*. Biotechnol. Bioeng. ***114***, 1025–1035.
37. Hu, Y., Zhu, Z., Nielsen, J., and Siewers, V. (2018). Heterologous transporter expression for improved fatty alcohol secretion in yeast. Metab. Eng. ***45***, 51–58.
38. Morel, D. (1983). Process for the Selective Addition of a Compound Having an Activated Carbon Atom onto a Substituted Conjugated Diene, [P].
39. Bian, G., Hou, A., Yuan, Y., et al. (2018). Metabolic engineering-based rapid characterization of a sesquiterpene cyclase and the skeletons of fusariumdiene and fusagramineol from *Fusarium graminearum*. Org. Lett. ***20***, 1626–1629.
40. Lian, J., Si, T., Nair, N.U., and Zhao, H. (2014). Design and construction of acetyl-CoA overproducing *Saccharomyces cerevisiae* strains. Metab. Eng. ***24***, 139–149.
41. Chen, H., Zhu, C., Zhu, M., et al. (2019). High production of valencene in *Saccharomyces cerevisiae* through metabolic engineering. Microb. Cell Fact. ***18***, 195.
42. Peng, B., Plan, M.R., Chrysanthopoulos, P., et al. (2017). A squalene synthase protein degradation method for improved sesquiterpene production in *Saccharomyces cerevisiae*. Metab. Eng. ***39***, 209–219.
43. Bian, G., Deng, Z., and Liu, T. (2017). Strategies for terpenoid overproduction and new terpenoid discovery. Curr. Opin. Biotechnol. ***48***, 234–241.
44. Siemon, T., Wang, Z., Bian, G., et al. (2020). Semisynthesis of plant-derived englerin A enabled by microbe engineering of guaia-6,10(14)-diene as building block. J. Am. Chem. Soc. ***142***, 2760–2765.
45. Son, Y.J., Kwon, M., Ro, D.K., and Kim, S.U. (2014). Enantioselective microbial synthesis of the indigenous natural product (-)-alpha-bisabolol by a sesquiterpene synthase from chamomile (*Matricaria recutita*). Biochem. J. ***463***, 239–248.
46. Picaud, S., Brodelius, M., and Brodelius, P.E. (2005). Expression, purification and characterization of recombinant (*E*)-beta-farnesene synthase from *Artemisia annua*. Phytochemistry ***66***, 961–967.
47. Bloom, J.D., Meyer, M.M., Meinhold, P., et al. (2005). Evolving strategies for enzyme engineering. Curr. Opin. Struct. Biol. ***15***, 447–452.
48. Arnold, F.H. (2019). Innovation by evolution: bringing new chemistry to life (Nobel Lecture). Angew. Chem. Int. Ed. Engl. ***58***, 14420–14426.
49. Leonard, E., Ajikumar, P.K., Thayer, K., et al. (2010). Combining metabolic and protein engineering of a terpenoid biosynthetic pathway for overproduction and selectivity control. Proc. Natl. Acad. Sci. U. S. A. ***107***, 13654–13659.
50. Flagfeldt, D.B., Siewers, V., Huang, L., and Nielsen, J. (2009). Characterization of chromosomal integration sites for heterologous gene expression in *Saccharomyces cerevisiae*. Yeast ***26***, 545–551.
51. Meadows, A.L., Hawkins, K.M., Tsegaye, Y., et al. (2016). Rewriting yeast central carbon metabolism for industrial isoprenoid production. Nature ***537***, 694–697.
52. Zhu, F., Lu, L., Fu, S., et al. (2015). Targeted engineering and scale up of lycopene overproduction in *Escherichia coli*. Process. Biochem. ***50***, 341–346.

ACKNOWLEDGMENTS

This work was financially supported by the National Key R&D Program of China (2018YFA0900400) and the National Natural Science Foundation of China (31670090). We also acknowledge Professor Zihe Liu from the Beijing University of Chemical Technology for kindly providing the pCas and KlURA3 plasmid.

AUTHOR CONTRIBUTIONS

T.L. conceived the idea of farnesene conversion to isophytol and organized teams to complete the work. Z.Y. performed the microbial synthesis experiments. K.S. was responsible for the chemical synthesis. T.L., Z.Y., and K.S. performed data analysis and wrote the manuscript. T.L. and Z.Y. edited the manuscript. B.S., Y.H., T.M., Z.X., Z.K., B.H., X.L., M.H., and Z.T. performed some experiments. Z.D. participated in the coordination and drafted the manuscript. All authors read and approved the final manuscript.

DECLARATION OF INTERESTS

The authors have applied for a series patents based on this work.

SUPPLEMENTAL INFORMATION

Supplemental information can be found online at https://doi.org/10.1016/j.xinn.2022.100228.

LEAD CONTACT WEBSITE

http://www.pharm.whu.edu.cn/info/1058/1639.htm.

The Innovation, Volume *3*

Supplemental Information

Revolution of vitamin E production by starting from microbial fermented farnesene to isophytol

Ziling Ye, Bin Shi, Yanglei Huang, Tian Ma, Zilei Xiang, Ben Hu, Zhaolin Kuang, Man Huang, Xiaoying Lin, Zhu Tian, Zixin Deng, Kun Shen, and Tiangang Liu

SUPPLEMENTAL INFORMATION

Supplemental Materials and Methods

Materials and reagents. PCR amplification for plasmid construction was performed using Phusion High-Fidelity polymerase (New England Biolabs, NEB) and Prime STAR GXL DNA polymerase (TaKaRa). A 2×Taq Plus Master Mix (Vazyme) was used for colony PCR diagnosis and error-prone PCR. PCR primers were synthesized by GeneGreate. Fast digestion restriction enzymes were purchased from Thermo Fisher Scientific. Enzymes for the Goldengate were purchased from New England Biolabs (NEB; Ipswich, MA, USA).

Strains and culture conditions. *Escherichia coli* DH10B was used to propagate the recombinant plasmids and was cultivated at 37 °C in Luria–Bertani (LB) medium containing 100 μg/mL ampicillin for selection. *S. cerevisiae* CEN.PK 2-1D was used as the host strain for farnesene-producing strains construction, and engineered yeast strains were selected at 30 °C on synthetic medium (0.67% yeast nitrogen base with $(NH_4)_2SO_4$, 2% glucose, and appropriate amino acid drop-out mix) under auxotroph-screening conditions (uracil 20 mg/L, histidine 20 mg/L, tryptophan 20 mg/L, and leucine 100 mg/L) or cultured in yeast extract–peptone–dextrose (YPD) medium (2% tryptone, 1% yeast extract, and 2% glucose) with antibiotic screening (hygromycin 200 mg/L). Synthetic medium supplemented with 1 g/L 5-fluoroorotic acid (5-FOA) was used to select positive colonies that lost the gRNA expression plasmid targeting the rDNA site. Agar was added to the medium at a concentration of 20 g/L, if a solid plate was needed.

Shake-flask fermentation. Seed cultures were prepared by inoculating glycerol stock into 5 mL of YPD medium or synthetic medium and cultured overnight at 30 °C in a rotary shaker at 220 rpm. Then seed cultures were transferred with initial OD_{600}= 0.1 into 250 mL shake flasks containing 50 mL corresponding medium, YPD or YPDHG (2% tryptone, 1% yeast extract, 1% glucose, and 1% galactose), or synthetic complete medium as described previously,[1] and 10 % v/v isopropyl myristate (IPM) was added into the medium to capture the farnesene. Flask cultivation was performed at 30 °C and 200 rpm for 72 h. All cultivations were performed in triplicates.

Construction of plasmids and strains. The strains and plasmids used in this study are listed in **Table S2, S3**. The primers used for plasmid construction are listed in **Table S4**. All heterologous genes used for gene screening were codon-optimized and synthesized by GenScript according to *S. cerevisiae* preference. The Golden Gate assembly,[2] Gibson method,[3] or yeast assembly[4] were used for plasmid construction. Gene deletion and genomic integrations for engineered yeast strain construction were conducted using the LiAc/SS carrier DNA/PEG method[5] and verified by diagnostic PCR.

Design and construction of farnesene synthase mutant libraries. Error-prone PCR using 2×Taq Plus Master Mix (Vazyme) with 6 mM additional Mg^{2+} was conducted to create the mutant libraries. The error-prone PCR fragments of bFS and vector bone pZY900 (*Bsa*I digested) were co-transformed to strain JCR27 to obtain farnesene synthase mutant libraries (**Figure 3**).

High-throughput cultivation and detection. Single colonies of recombinant yeast

strains harboring plasmids with different site-mutations of farnesene synthase were inoculated into 96-deep well microtiter plates with 350 μL Sc-ura medium and cultured for 24 h at 30 °C in a rotary shaker at 999 rpm. To avoid the edge effect, the same volume of medium was added to the outer margin of the 96-deep well plate without inoculation. The seed broth was transferred into 350 μL YPDHG with 20% v/v IPM overlay and grown for 72 h. IPM (200 μL) was added to each well to extract the product with 999 rpm shaking for 10 min, and the microtiter plate was centrifuged at 3500 rpm for 10 min. The organic phase (15 μL) was transferred into a 96-well plate; 120 μL of 75% H_2SO_4 and 15 μL of 8 mg/mL vanillin aqueous solution were added and the samples were incubated at 65 °C for 20 min in a rotary shaker at 999 rpm. The absorbance was measured at 454 nm using a plate reader. Strains with high absorbance were chosen for further shake flask fermentation to ensure actual improvement compared to the wild type. Positive mutants were cultured for plasmid extraction and sequencing.

Fed-batch fermentation. One-liter bioreactors (T&J Bio-engineering Co., Ltd.) were used to evaluate the performance of the engineered strains. The fermentation medium used in this study was based on a previously described medium.[6,7,8] The medium for the batch phase contained (per L): glucose, 40 g; $(NH_4)_2SO_4$, 15 g; KH_2PO_4, 8.0 g; and $MgSO_4 \cdot 7H_2O$, 6.2 g. The medium was sterilized in the fermenter at 115 °C for 30 min. After sterilization, 12 mL/L trace metal solution and 15 mL/L vitamin solution were added. Feeding solution I contained 500 g/L glucose, 9 g/L KH_2PO_4, 5.2 g/L $MgSO_4 \cdot 7H_2O$, 3.5 g/L K_2SO_4, 0.28 g/L Na_2SO_4, 12 mL/L trace metal solution, and 15 mL/L vitamin solution. Feeding solution II contained 800 g/L sucrose, 9 g/L KH_2PO_4, 5.2 g/L $MgSO_4 \cdot 7H_2O$, 3.5

g/L K_2SO_4, 0.28 g/L Na_2SO_4, 12 mL/L trace metal solution, and 15 mL/L vitamin solution. The concentrated trace metal solution contained (per L): ethylenediaminetetraacetic acid (EDTA), 15 g; $ZnSO_4 \cdot 7H_2O$, 5.75 g; $MnCl_2 \cdot 4H_2O$, 0.32 g; $CuSO_4 \cdot 5H_2O$, 0.75 g; $CoCl_2 \cdot 6H_2O$, 0.47 g; $Na_2MoO_4 \cdot 2H_2O$, 0.48 g; $CaCl_2 \cdot 2H_2O$, 2.9 g; and $FeSO_4 \cdot 7H_2O$, 2.8 g. The vitamin solution contained (per L): biotin, 0.1 g; calcium pantothenate, 3.0 g; nicotinic acid, 1.0 g; myo-inositol, 25.0 g; thiamine hydrochloride, 1.5 g; pyridoxol hydrochloride, 1 g; and p-aminobenzoic acid, 0.2 g. The trace metal and vitamin solutions were filter-sterilized before use. Seed cultures were prepared by inoculating glycerol stock into 5 mL of YPD medium and cultured overnight at 30 ºC in a rotary shaker at 220 rpm. Then, 10 % seed cultures were transferred into 250 mL shake flasks containing 50 mL YPD and cultured at 30 ºC with shaking at 220 rpm for 14 h; 10% of the seed culture was then inoculated into 350 mL fermentation medium in a 1 L fermenter for fed-batch fermentation at 30 ºC, with the pH maintained at 5 using ammonia. Fermentation was performed at an agitation speed of between 200 rpm and 600 rpm and an airflow rate ranging from 0.2 vvm to 2 vvm to hold the DO beyond 20%. Similarly, a two-phase culture system using IPM was applied for farnesene production.

GC/MS detection of β-farnesene. The organic phase of the two-phase culture was collected and centrifuged for 10 min at 3500 rpm to remove cell debris and diluted with hexane to an appropriate range. Samples were then subjected to gas chromatography–mass spectrometry (GC-MS) to quantify the concentration of farnesene using a Thermo Fisher Scientific TSQ QUANTUM XLS with a TR-5MS column (30 m × 0.25 mm × 0.25 μm). The oven temperature was initially held at 50 ºC for 1 min, increased

at a rate of 15 ºC/min to 280 ºC holding on for 1 min, then increased to 300 ºC at a rate of 20 °C/min, and held for 2 min. β-farnesene in hexane was used as the calibration standard, and valencene was used as an internal standard.

Lycopene extraction and quantitation. 100 μL of the sampled culture was centrifuged at 12,000 rpm for 2 min in a 2-mL tube, and the supernatant was discarded. Then, 200 μL glass beads (diameter, 0.5 mm) were added to the pelleted cells, vortexed for 3 min to lyse the cell, extracted with acetone in the dark, and centrifuged at 13,000 for 5 min. The supernatant was then transferred to sample vials for HPLC analysis. An HPLC instrument (Thermo Fisher Scientific) equipped with a UV detector and an Agilent Zorbax C18 column (150 mm × 4.6 mm × 5 μm) was used for lycopene analysis. The absorption wavelength of lycopene was 474 nm. Mobile phases A (acetonitrile/water = 9:1, v/v) and B (methanol/isopropanol = 3:2, v/v) were eluted as follows: 0%–90% B (0−15 min), 90% B (15−30 min), and 90%−0% B (30−35 min), with a flow rate of 1 mL/min.

Synthetic procedure of isophytol from β-farnesene.

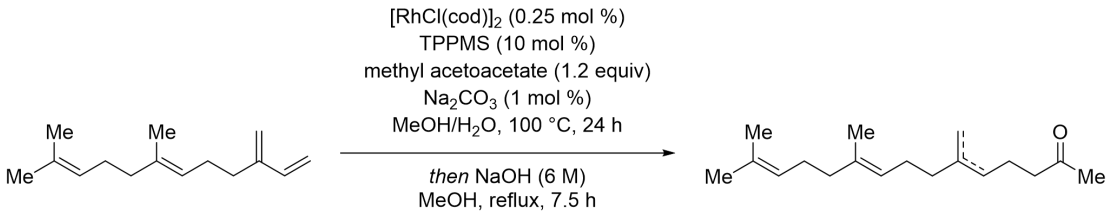

β-Farnesene
(10 mmol)

1
95% yield

A Schlenk tube was charged with $[RhCl(cod)]_2$ (12.6 mg, 0.025 mmol), TPPMS (364.2 mg, 1 mmol), and Na_2CO_3 (10.7 mg, 0.1 mmol). The tube was degassed and refilled with N_2 three times. Then, β-farnesene (2.4 mL, 10 mmol), methyl acetoacetate (1.3 mL, 12 mmol), MeOH (5 mL) and H_2O (5 mL) were added *via* syringe under N_2. The resulting

mixture was stirred at 100 °C for 24 h, cooled to room temperature, and extracted with EtOAc. The combined extracts were dried over Na_2SO_4, filtered, and concentrated. The residue was dissolved in an aqueous solution of NaOH (6 M in H_2O, 12 mL). MeOH (30 mL) was added to the mixture. The resulting mixture was stirred under reflux for 7.5 h, cooled to room temperature, and extracted with EtOAc. The combined extracts were filtered through a pad of silica gel. The filtrate was concentrated under reduced pressure to provide **1** as a mixture of two inseparable regioisomers (2.49 g, 95% yield, 65:35 ratio). ^{1}H NMR (400 MHz, $CDCl_3$): δ 5.17–5.06 (m, 2.35H), 4.73 (s, 0.65H), 4.71 (s, 0.65H), 2.46–2.40 (m, 2.00H), 2.25 (dd, *J* = 14.8, 7.6 Hz, 0.70H), 2.12–1.96 (m, 12.30H), 1.74–1.67 (m, 4.30H), 1.60–1.58 (m, 7.05H); ^{13}C NMR (100 MHz, $CDCl_3$): δ 208.8, 148.5, 136.2, 135.1, 134.9, 131.1, 124.3, 124.2, 123.9, 123.8, 122.4, 109.5, 43.6, 42.9, 39.61, 39.59, 39.5, 35.7, 35.2, 29.8, 26.63, 26.56, 26.4, 26.1, 25.6, 22.3, 21.5, 17.6, 15.90, 15.86.

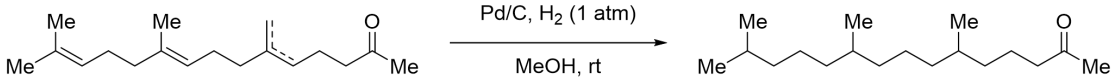

1 **2**

98% yield

To a 50 mL round-bottom flask was added 10% Pd/C (157.5 mg), **1** (788.0 mg, 3 mmol), and MeOH (15 mL) under N_2. An atmosphere of hydrogen was introduced by briefly evacuating the flask and flushing with H_2 gas (1 atm, hydrogen balloon). The mixture was stirred at room temperature overnight under H_2 atmosphere. The hydrogen was then removed under vacuum and the flask was refilled with nitrogen. The mixture was filtered through a pale of Celite, and the filtrate was concentrated under reduced pressure to

obtain **2** as a colorless oil (785.7 mg, 98% yield); ^{1}H NMR (400 MHz, $CDCl_3$): δ 2.39 (t, *J* = 7.6 Hz, 2H), 2.12 (s, 3H), 1.62–1.47 (m, 3H), 1.36–1.31 (m, 2H), 1.30–1.16 (m, 8H), 1.14–0.99 (m, 6H), 0.86–0.82 (m, 12H); ^{13}C NMR (100 MHz, $CDCl_3$): δ 209.2, 44.0, 39.3, 37.31, 37.29, 37.26, 37.2, 37.14, 37.09, 36.5, 36.4, 32.69, 32.67, 32.58, 32.56, 29.7, 29.6, 27.9, 24.73, 24.71, 24.3, 22.6, 22.5, 21.3, 19.7, 19.6, 19.5, 19.4.

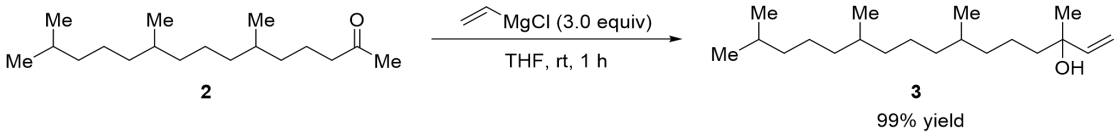

2 **3**

99% yield

A 100 mL round-bottom flask was charged with **2** (796.0 mg, 3 mmol). The flask was degassed and refilled with N_2 three times. Then, THF (30 mL) and vinyl magnesium chloride (1.0 M solution in THF, 9 mL, 3 equiv) were added under N_2. The resulting mixture was stirred at room temperature for 1 h and then quenched by the addition of a saturated aqueous solution of NH_4Cl. The organic layer was separated, and the aqueous layer was extracted with EtOAc. The combined organic layers were dried over Na_2SO_4 and filtered. The filtrate was concentrated under reduced pressure to obtain **3** as a colorless oil (880.7 mg, 99% yield). ^{1}H NMR (400 MHz, $CDCl_3$): δ 5.91 (dd, *J* = 17.2, 10.8 Hz, 1H), 5.19 (d, *J* = 18.4 Hz, 1H), 5.03 (d, *J* = 10.8 Hz, 1H), 1.55–1.45 (m, 4H), 1.38–1.33 (m, 3H), 1.31–1.19 (m, 13H), 1.15–1.11 (m, 2H), 1.10–1.03 (m, 4H), 0.86 (s, 3H), 0.85 (s, 3H), 0.84 (s, 3H), 0.82 (s, 3H); ^{13}C NMR (100 MHz, $CDCl_3$): δ 145.24, 145.22, 111.4, 73.3, 42.7, 39.3, 37.5, 37.4, 37.3, 37.2, 32.74, 32.72, 27.9, 27.63, 27.60, 24.77, 24.76, 24.4, 22.7, 22.6, 21.33, 21.31, 19.7, 19.63, 19.59.

Synthesis of Farnesyl Acetone from α-Farnesene.

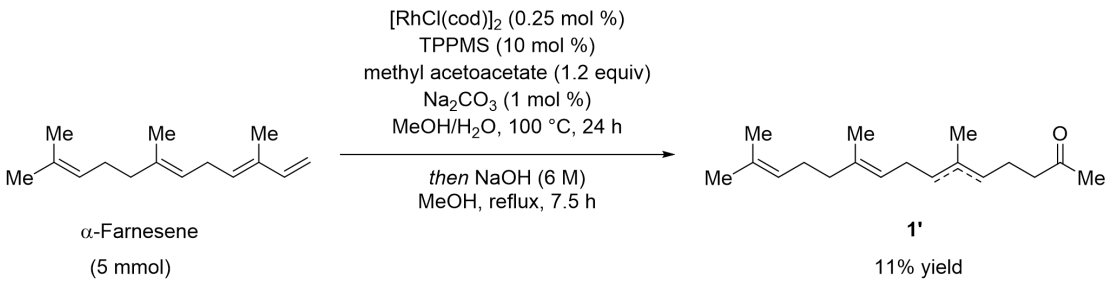

α-Farnesene
(5 mmol)

1'
11% yield

A Schlenk tube was charged with $[RhCl(cod)]_2$ (6.2 mg, 0.0125 mmol), TPPMS (182.2 mg, 0.5 mmol), and Na_2CO_3 (5.3 mg, 0.05 mmol). The tube was degassed and refilled with N_2 three times. Then α-farnesene (1.2 mL, 5 mmol), methyl acetoacetate (0.65 mL, 6 mmol), MeOH (2.5 mL), and H_2O (2.5 mL) were added *via* syringe under N_2. The resulting mixture was allowed to stirred at 100 °C for 24 h, cooled to room temperature, and extracted with EtOAc. The combined extracts were dried over Na_2SO_4, filtered, and concentrated. The residue was dissolved in an aqueous solution of NaOH (6 M in H_2O, 6 mL). MeOH (15 mL) was added to the mixture. The resulting mixture was stirred under reflux for 7.5 h, cooled to room temperature, and extracted with EtOAc. The combined extracts were filtered through a pad of silica gel. Purification by column chromatography (5% EtOAc in petroleum ether) gave **1'** as a mixture of two inseparable regioisomers (141.1 mg, 11% yield, 65:35 ratio). ^{1}H NMR (400 MHz, $CDCl_3$): δ 5.20–5.00 (m, 3H), 2.68 (t, *J* = 7.2 Hz, 1.30H), 2.44 (t, *J* = 7.2 Hz, 0.70H), 2.38 (t, *J* = 7.2 Hz, 1.30H), 2.26 (t, *J* = 7.2 Hz, 0.70H), 2.13 (s, 1.05H), 2.12 (s, 1.95H), 2.10–1.92 (m, 7H), 1.75–1.55 (m, 13H); ^{13}C NMR (100 MHz, CDCl3): δ 209.3, 208.9, 136.5, 135.2, 135.0, 134.0, 131.3, 124.2, 124.1, 123.9, 123.2, 122.9, 43.9, 42.9, 39.7, 39.6, 39.7, 39.7, 31.8, 30.0, 29.9, 26.8, 26.6, 26.3, 25.6, 23.3, 22.2, 21.7, 17.6, 16.0, 15.9, 15.7.

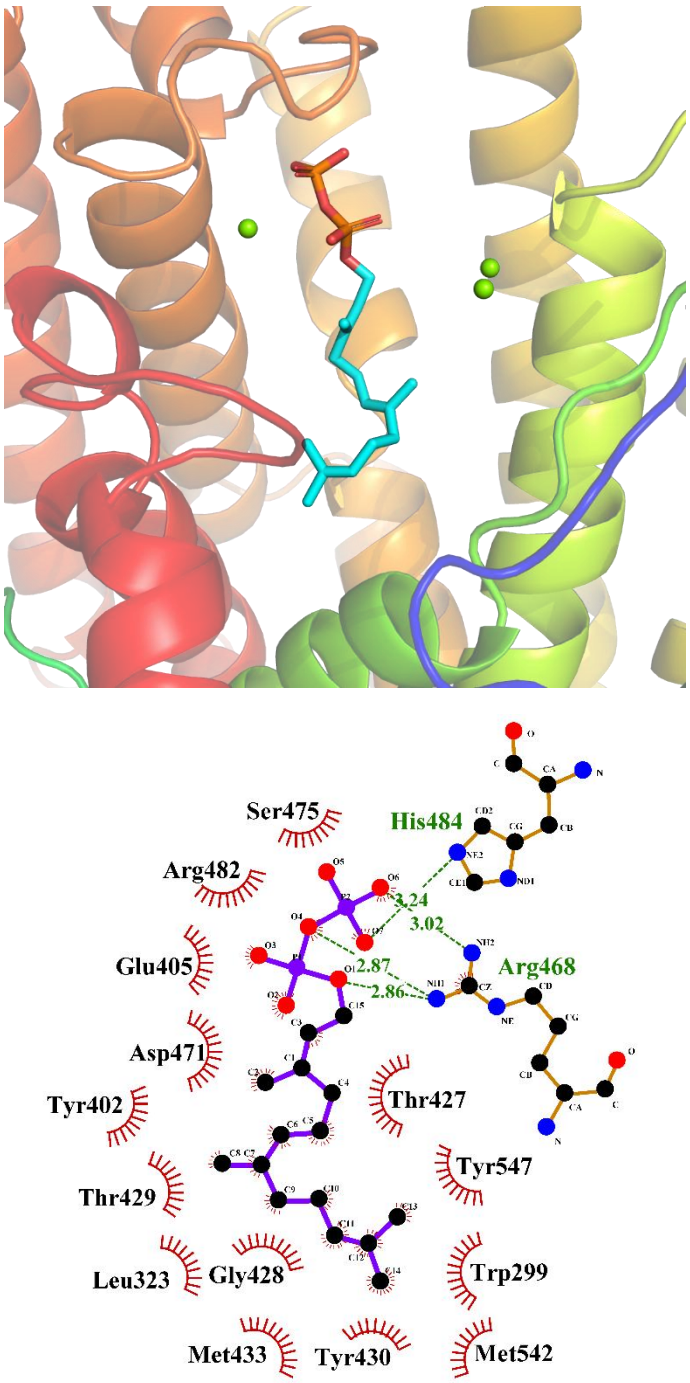

Figure S1. The 3D structure (upper) and 2D interaction map (bottom) between simulated BFS1 (wild-type) and farnesyl diphosphate (FPP). The red arcs with rays denote hydrophobic contacts, green dashed lines denote putative hydrogens bonds and metal contacts, and numbers over the dashed lines denote the distance (Å).

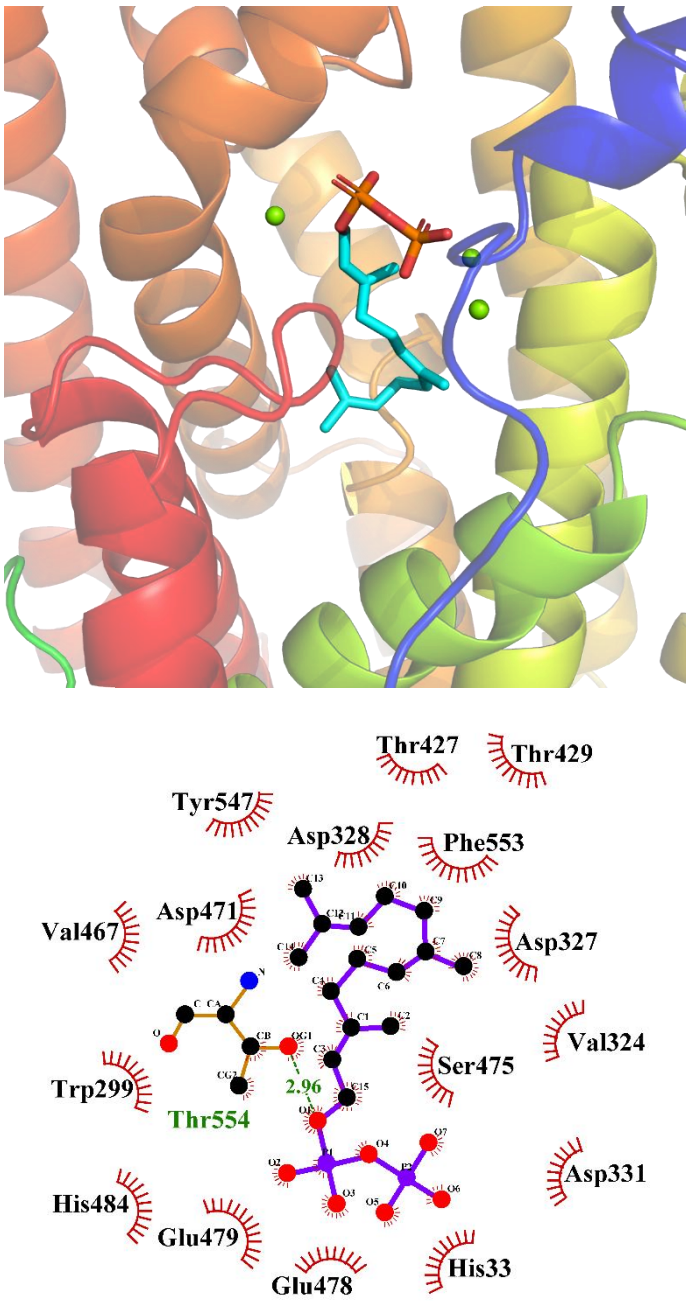

Figure S2. The 3D structure (upper) and 2D interaction map (bottom) between simulated BFS9 (F11S mutation) and farnesyl diphosphate (FPP). The red arcs with rays denote hydrophobic contacts, green dashed lines denote putative hydrogens bonds and metal contacts, and numbers over the dashed lines denote the distance (Å).

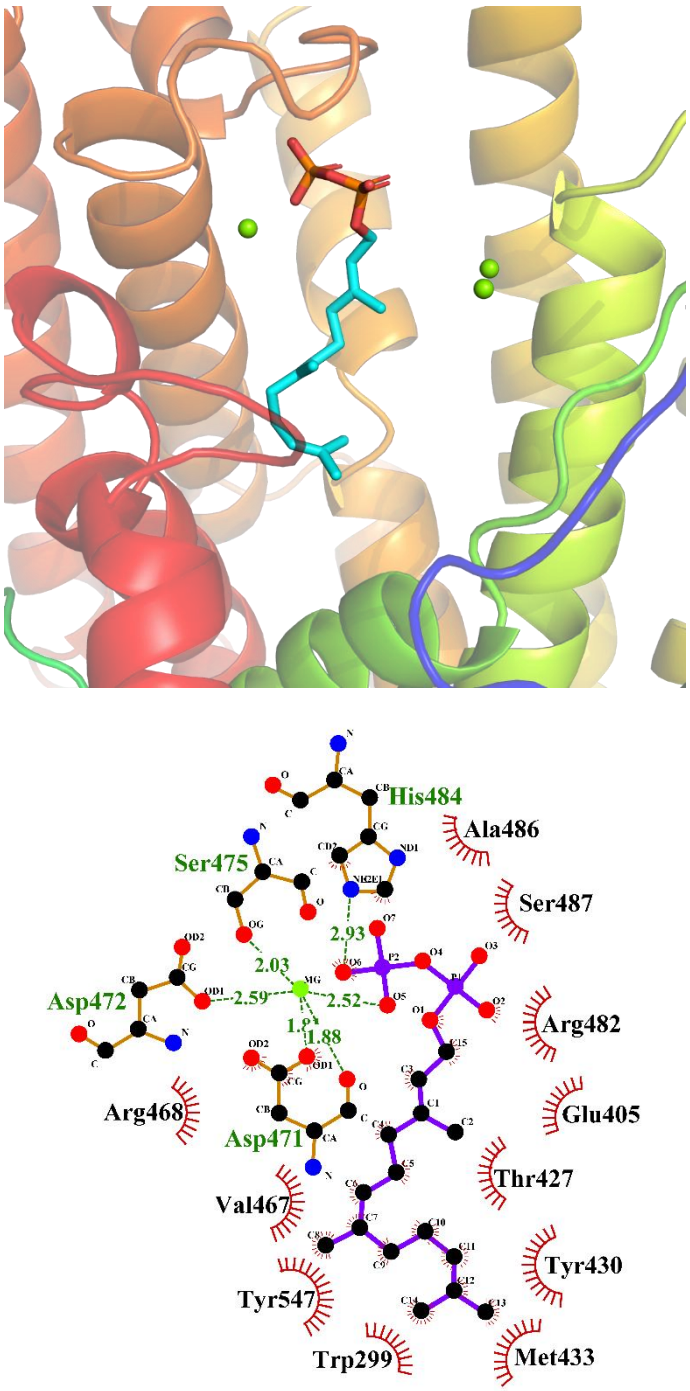

Figure S3. The 3D structure (upper) and 2D interaction map (bottom) between simulated BFS12 (M35T mutation) and farnesyl diphosphate (FPP). The red arcs with rays denote hydrophobic contacts, green dashed lines denote putative hydrogens bonds and metal contacts, and numbers over the dashed lines denote the distance (Å).

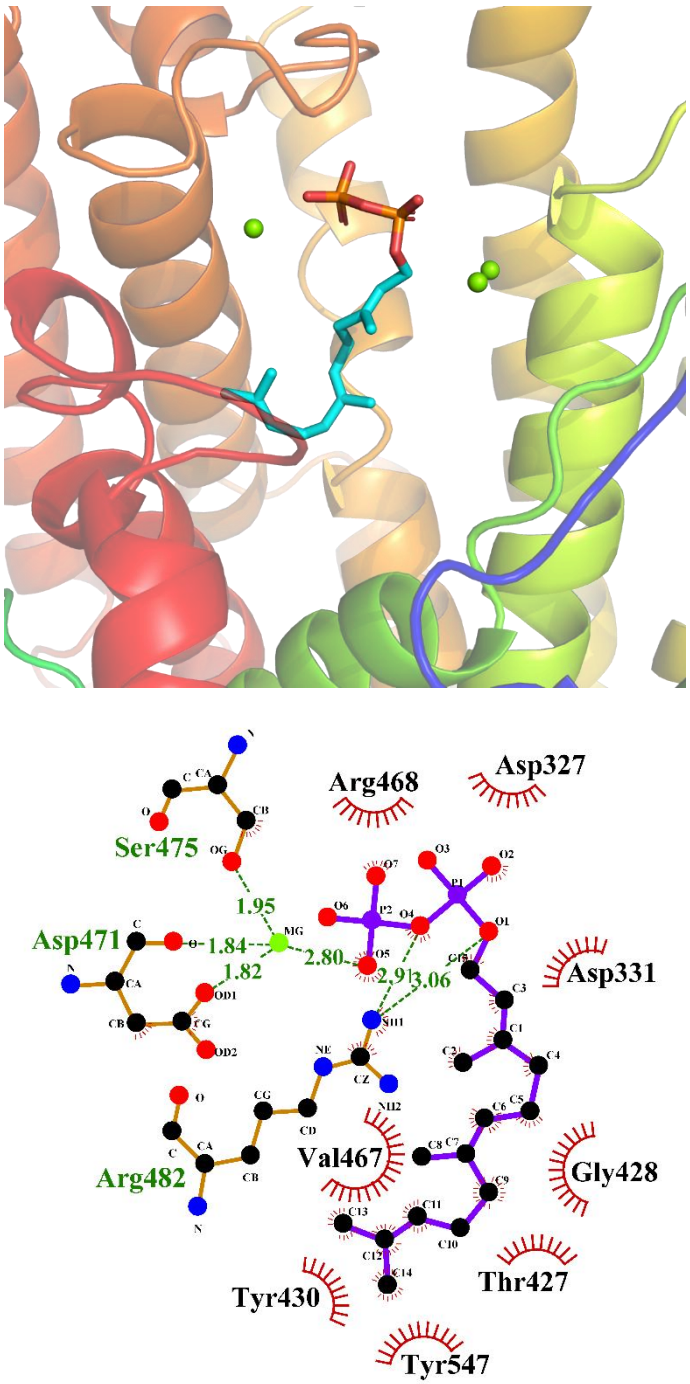

Figure S4. The 3D structure (upper) and 2D interaction map (bottom) between simulated BFS15 (T319S mutation) and farnesyl diphosphate (FPP). The red arcs with rays denote hydrophobic contacts, green dashed lines denote putative hydrogens bonds and metal contacts, and numbers over the dashed lines denote the distance (Å).

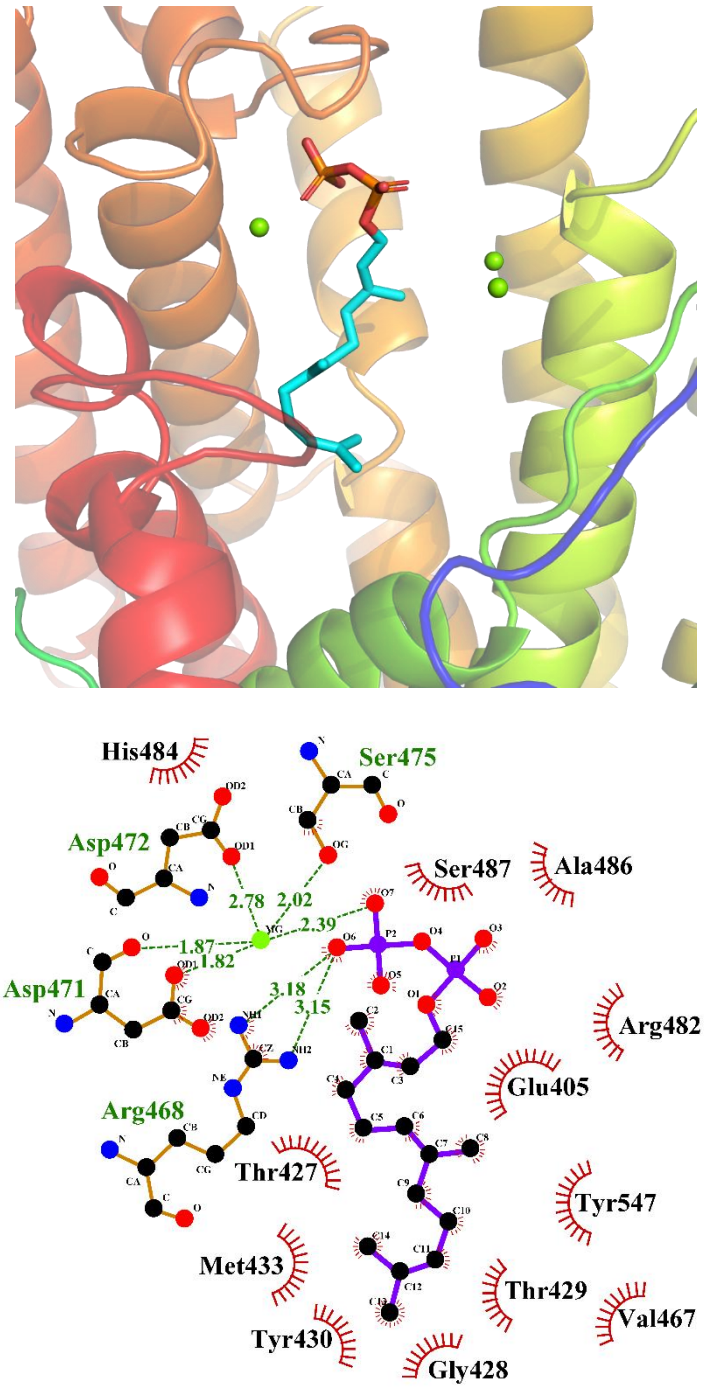

Figure S5. The 3D structure (upper) and 2D interaction map (bottom) between simulated BFS18 (I434T mutation) and farnesyl diphosphate (FPP). The red arcs with rays denote hydrophobic contacts, green dashed lines denote putative hydrogens bonds and metal contacts, and numbers over the dashed lines denote the distance (Å).

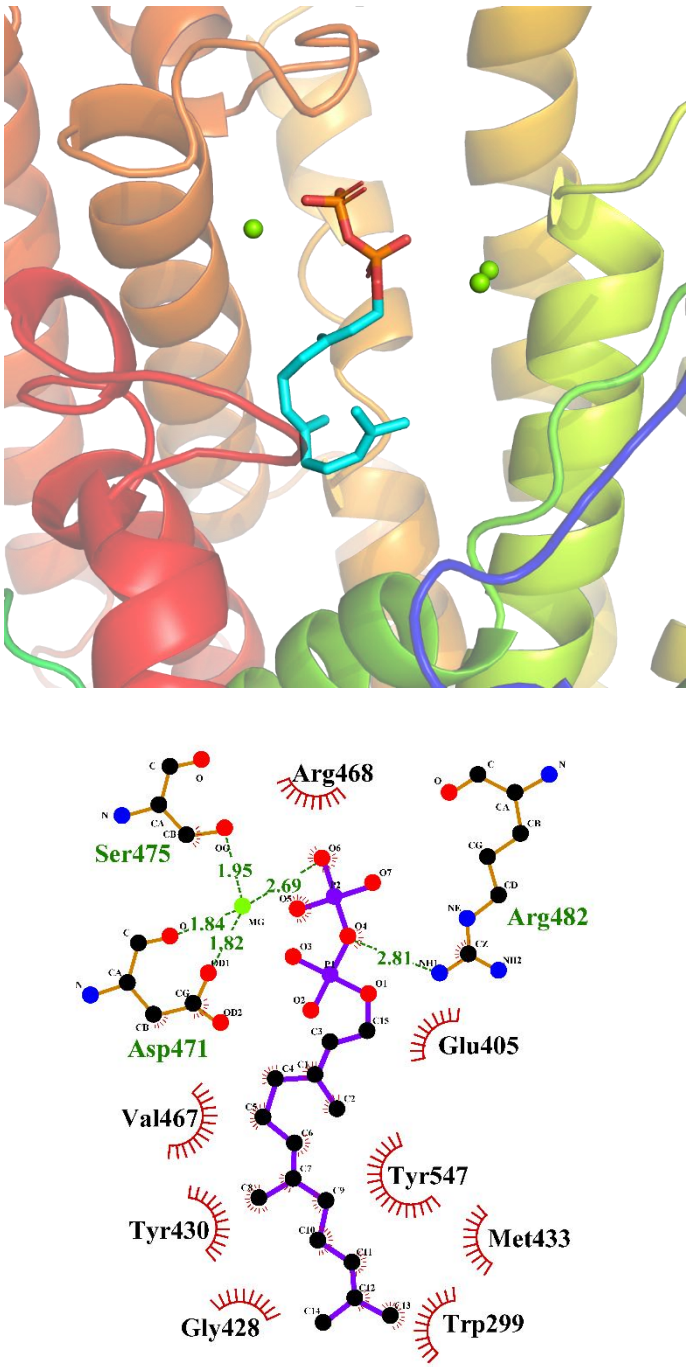

Figure S6. The 3D structure (upper) and 2D interaction map (bottom) between simulated BFS20 (I460V mutation) and farnesyl diphosphate (FPP). The red arcs with rays denote hydrophobic contacts, green dashed lines denote putative hydrogens bonds and metal contacts, and numbers over the dashed lines denote the distance (Å).

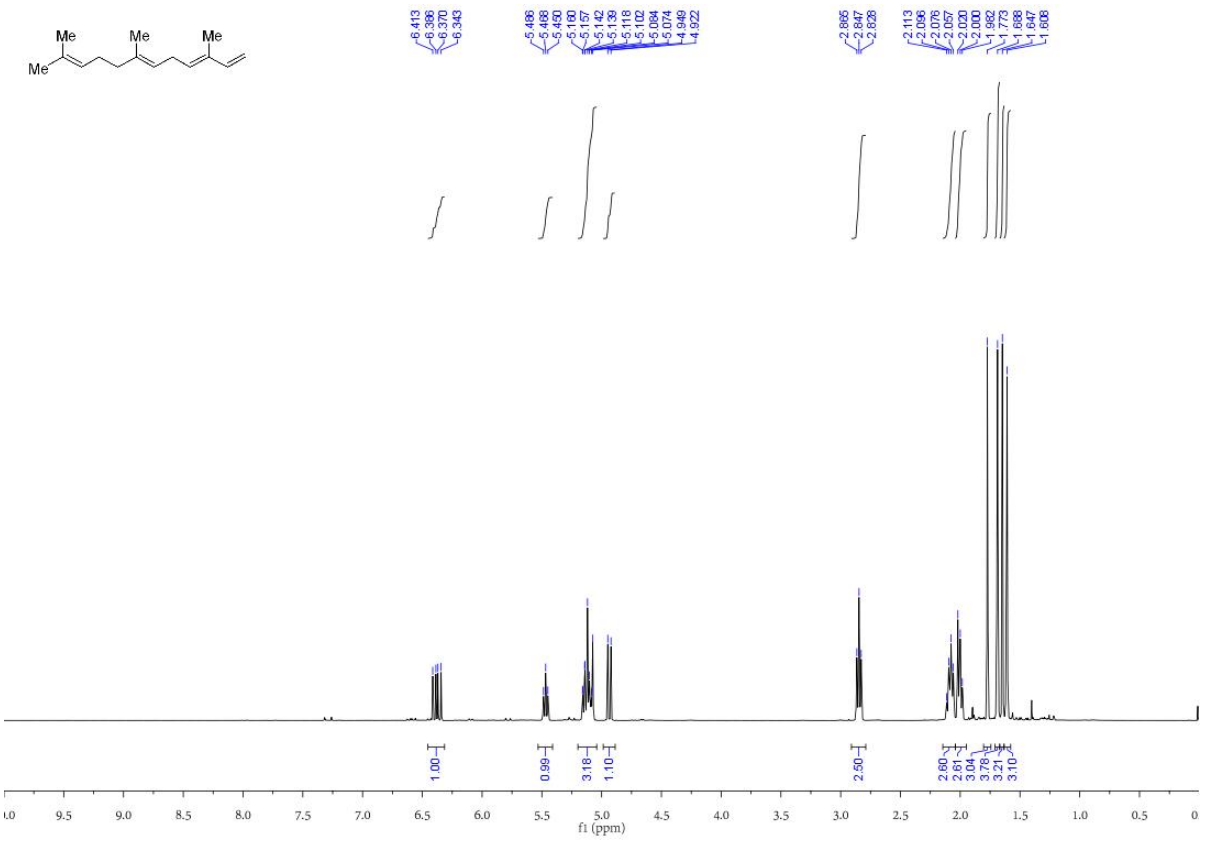

Figure S7. ^{1}H NMR spectrum of biosynthetic α-farnesene.

^{1}H NMR (400 MHz, $CDCl_3$): δ 6.38 (dd, *J* = 17.2, 10.8 Hz, 1H), 5.46 (t, *J* = 7.2 Hz, 1H), 5.18–5.05 (m, 2H), 5.10 (d, *J* = 17.2 Hz, 1H), 4.93 (d, *J* = 10.8 Hz, 1H), 2.84 (t, *J* = 7.2 Hz, 2H), 2.15–2.05 (m, 2H), 2.05–1.95 (m, 2H), 1.77 (s, 3H), 1.68 (s, 3H), 1.64 (s, 3H), 1.60 (s, 3H).

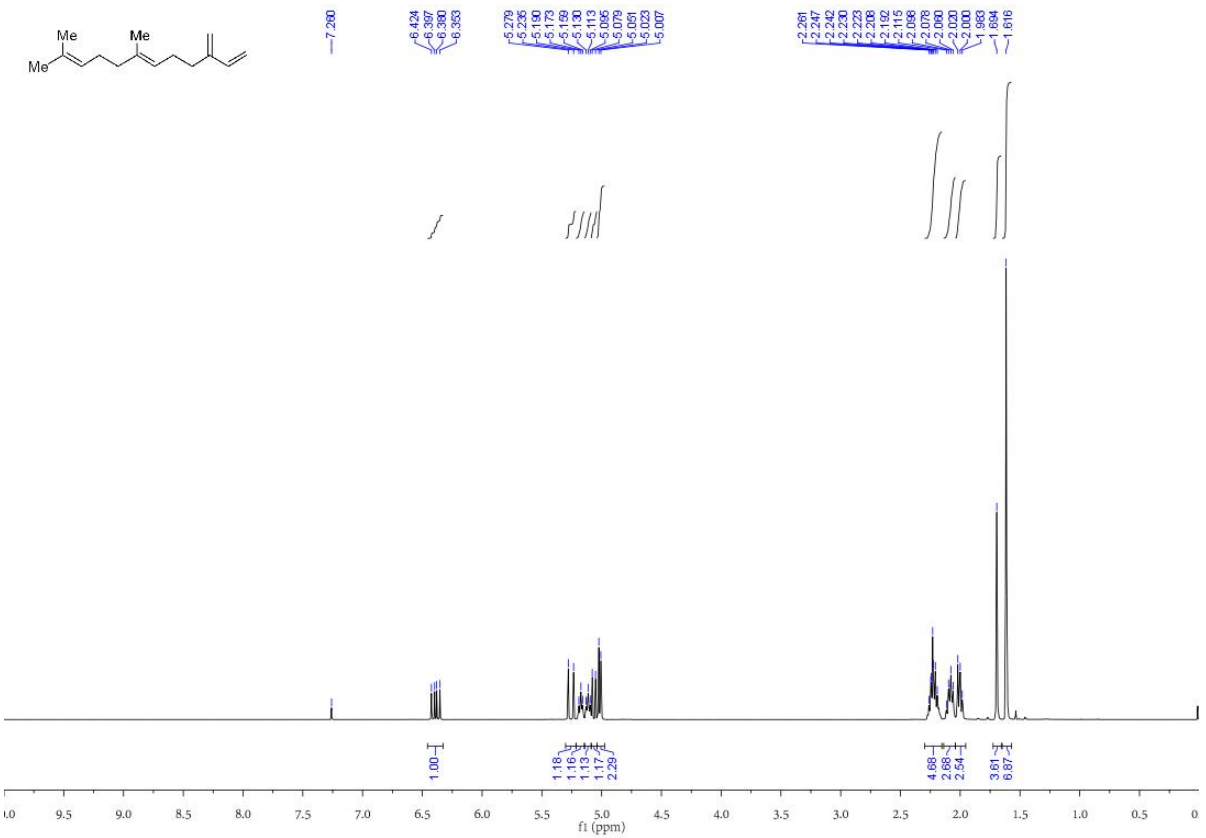

Figure S8. ^{1}H NMR spectrum of biosynthetic β-farnesene.

^{1}H NMR (400 MHz, $CDCl_3$): δ 6.39 (dd, *J* = 17.6, 10.8 Hz, 1H), 5.26 (d, *J* = 17.6 Hz, 1H), 5.21–5.14 (m, 1H), 5.14–5.08 (m, 1H), 5.06 (d, *J* = 10.8 Hz, 1H), 5.02 (s, 1H), 5.00 (s, 1H), 2.30–2.15 (m, 4H), 2.15–2.05 (m, 2H), 2.05–1.95 (m, 2H), 1.69 (s, 3H), 1.61 (s, 6H).

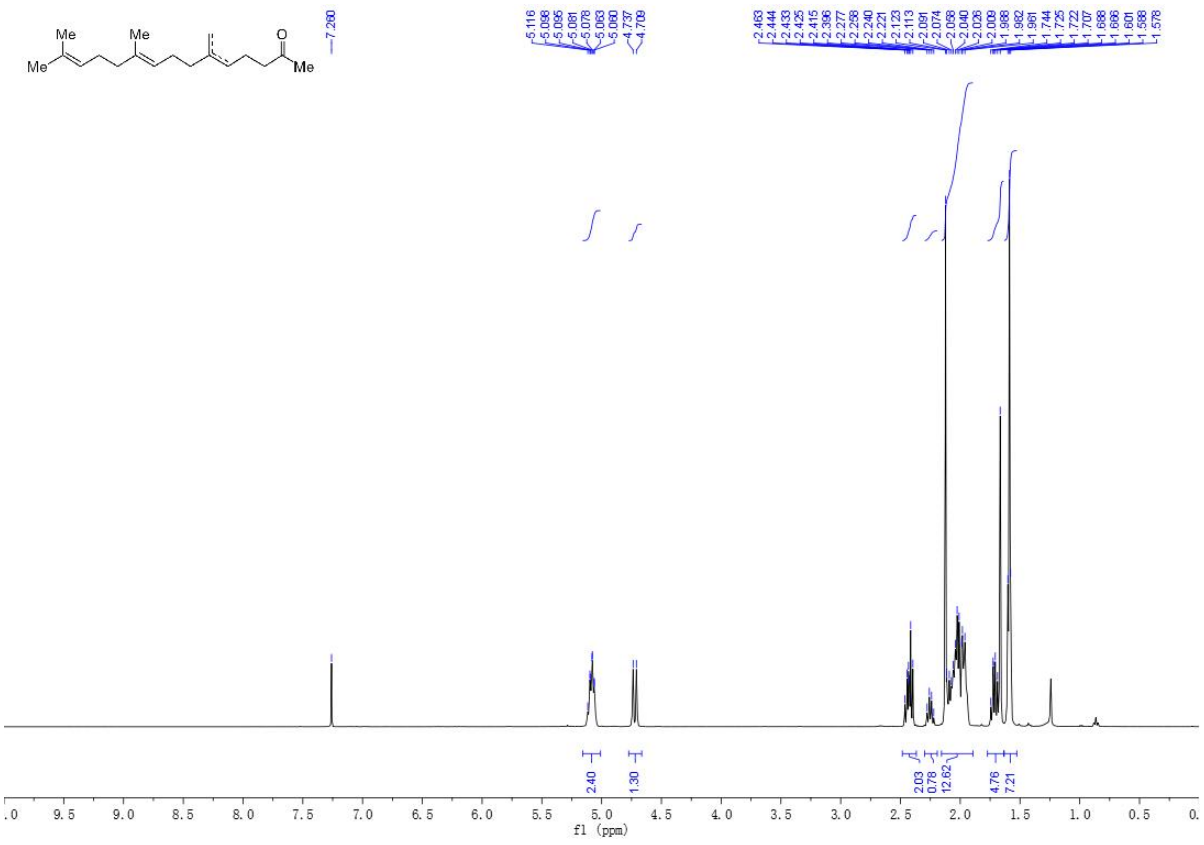

Figure S9. ^{1}H NMR spectrum of compound 1.

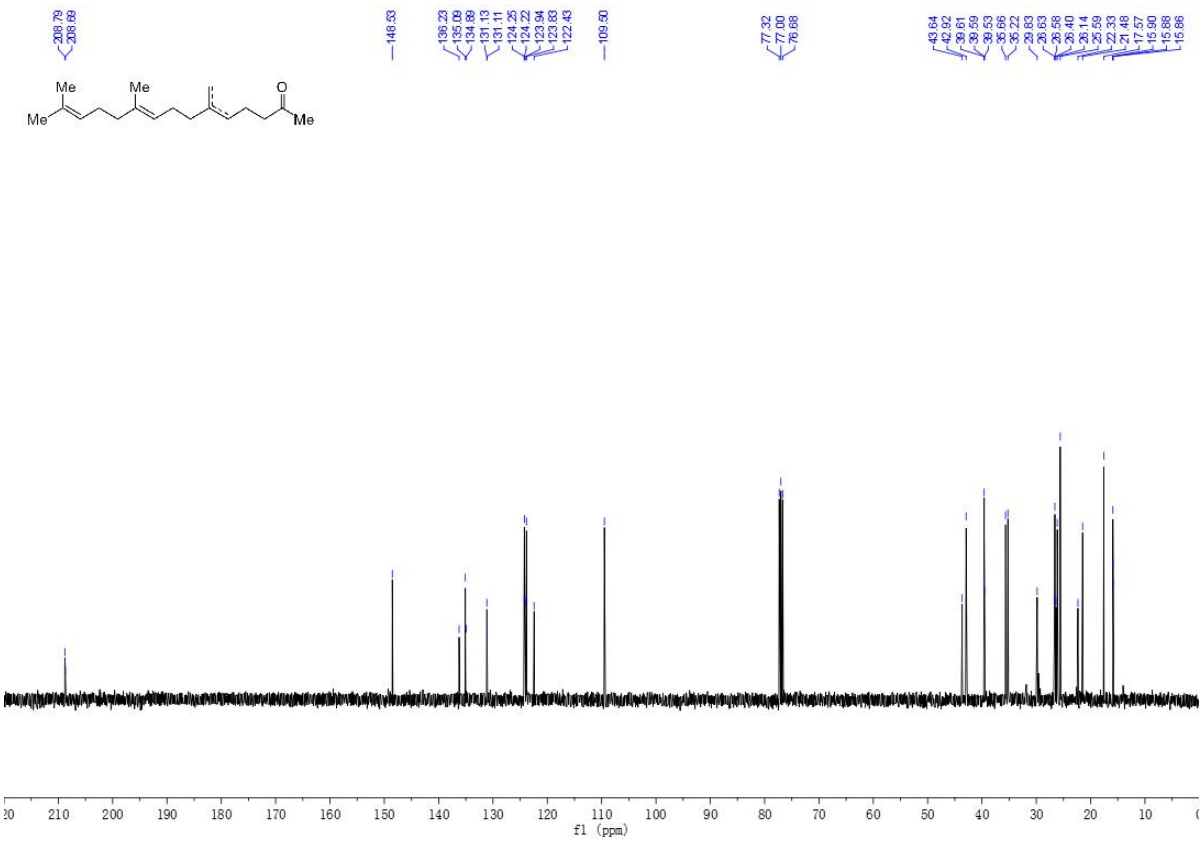

Figure S10. ^{13}C NMR spectrum of compound 1.

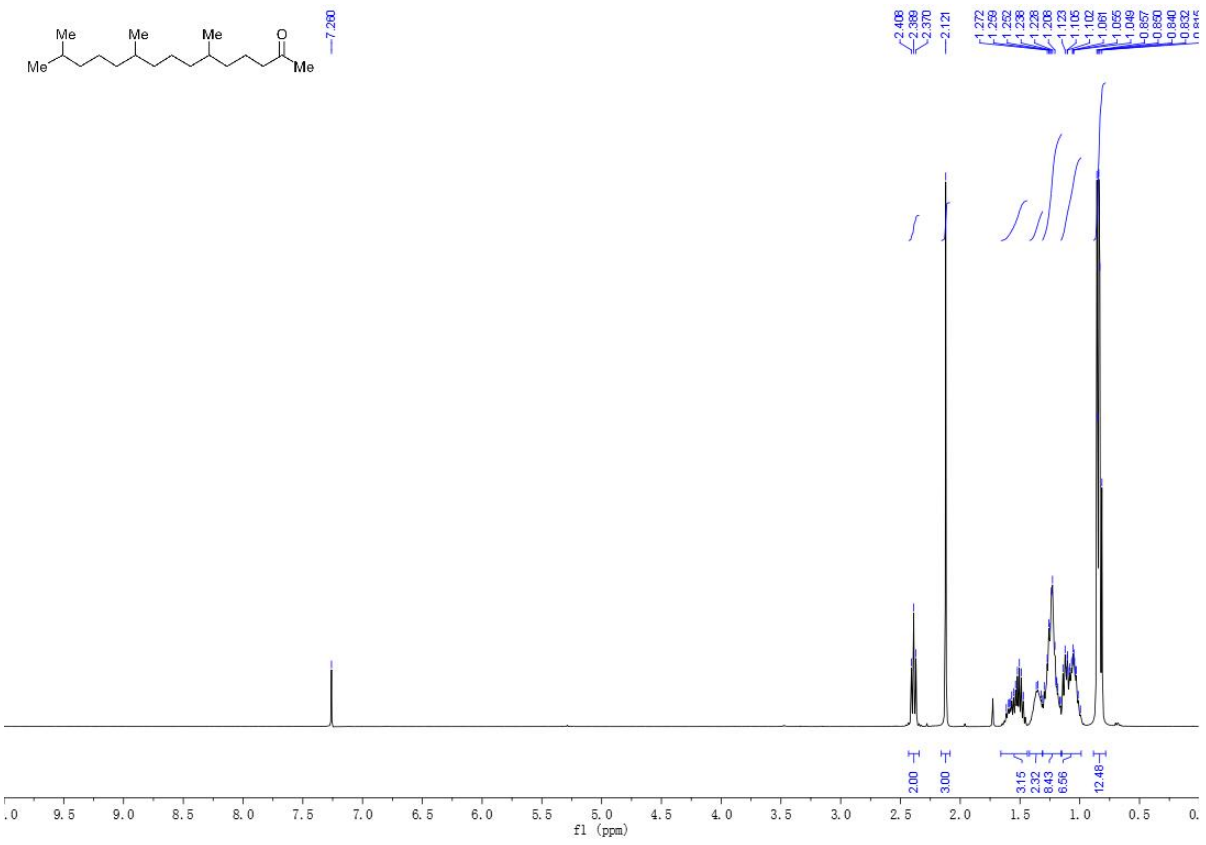

Figure S11. ^{1}H NMR spectrum of compound 2.

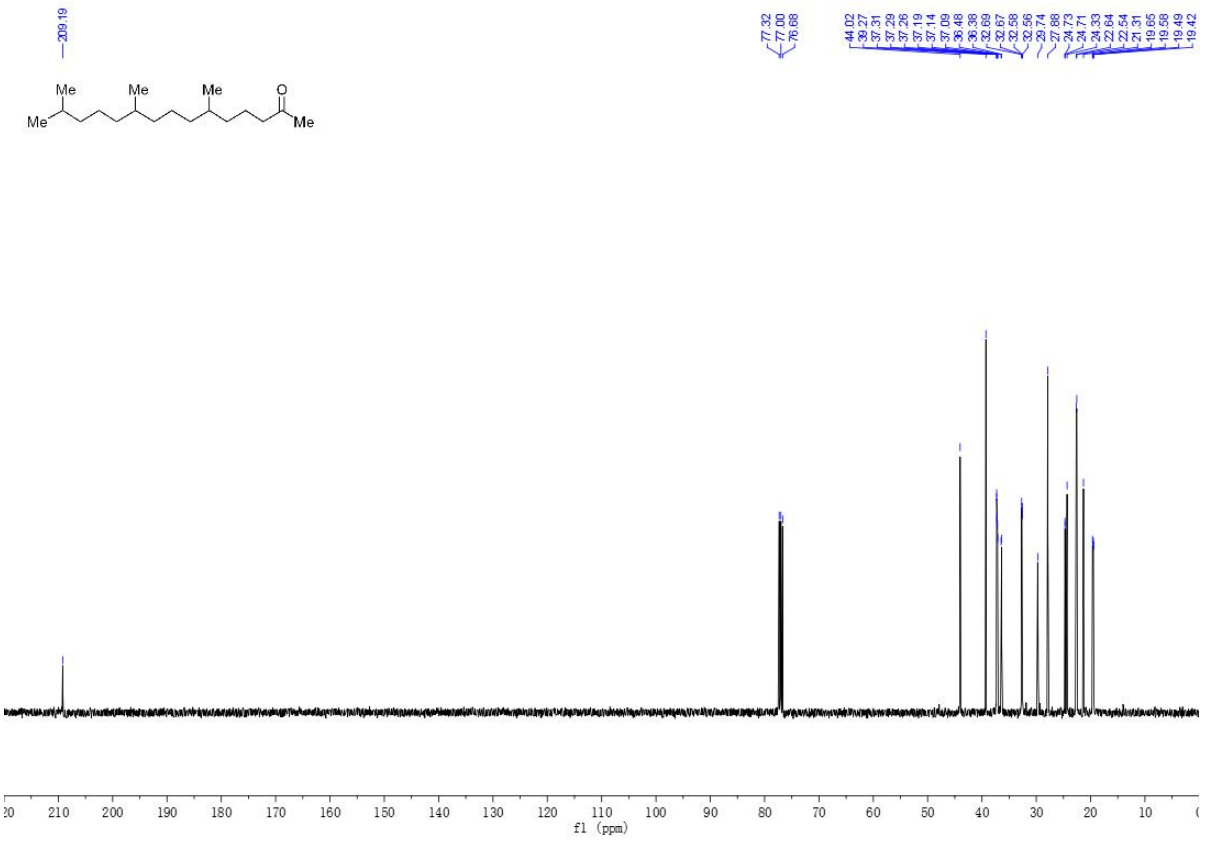

Figure S12. ^{13}C NMR spectrum of compound 2.

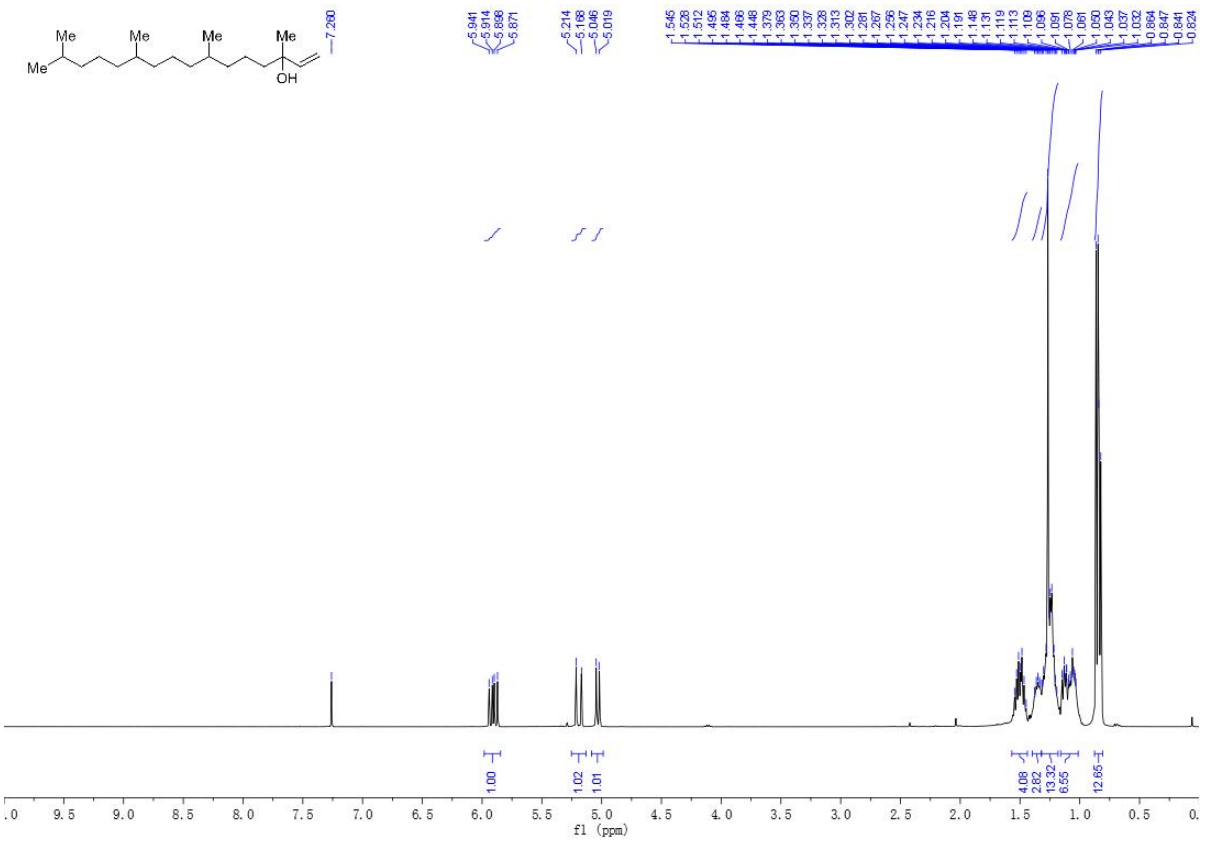

Figure S13. ^{1}H NMR spectrum of compound 3.

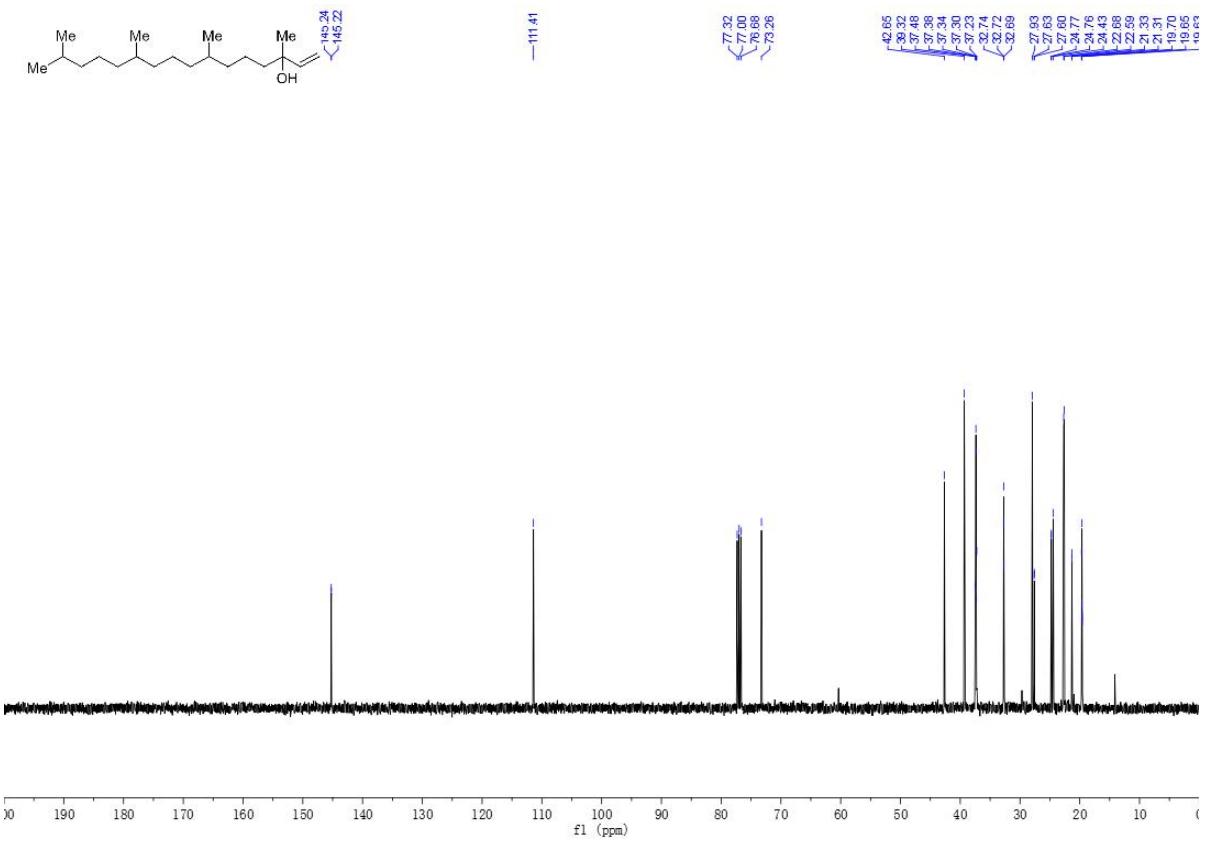

Figure S14. ^{13}C NMR spectrum of compound 3.

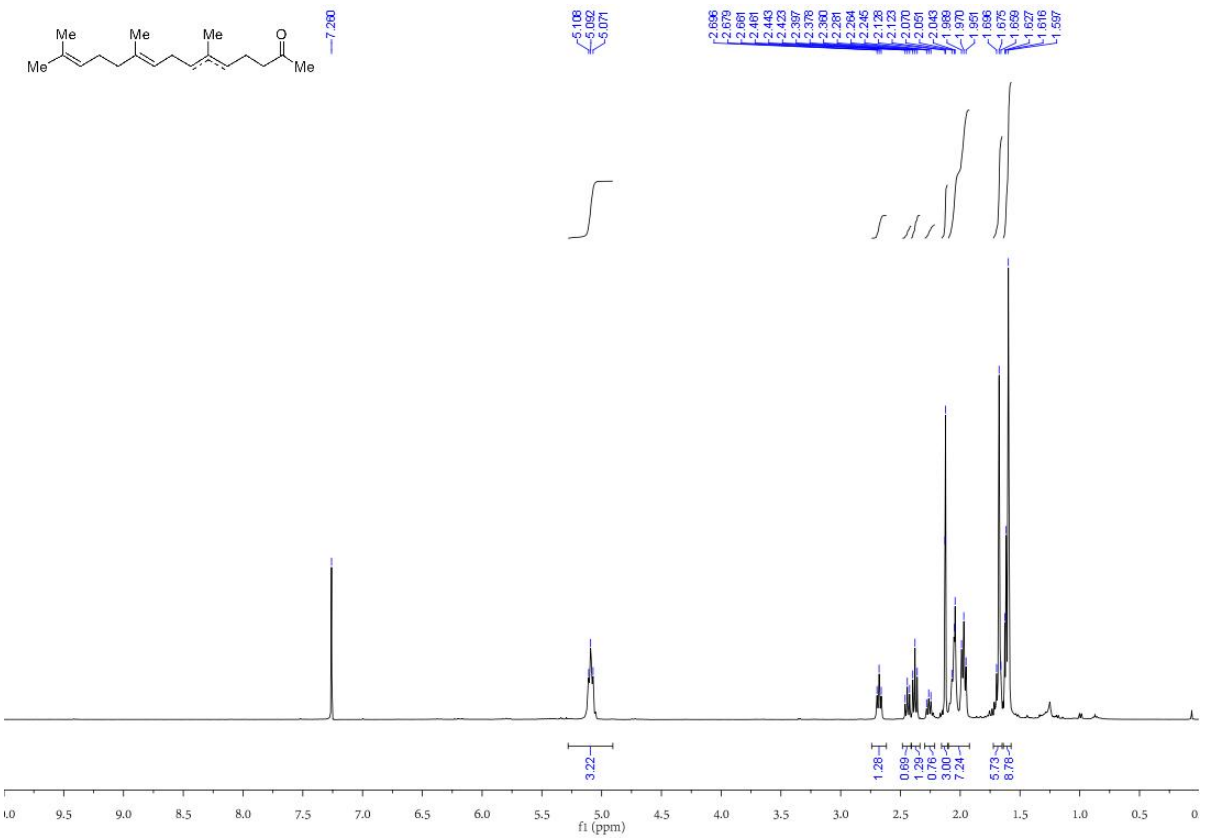

Figure S15. ^{1}H NMR spectrum of compound 1'.

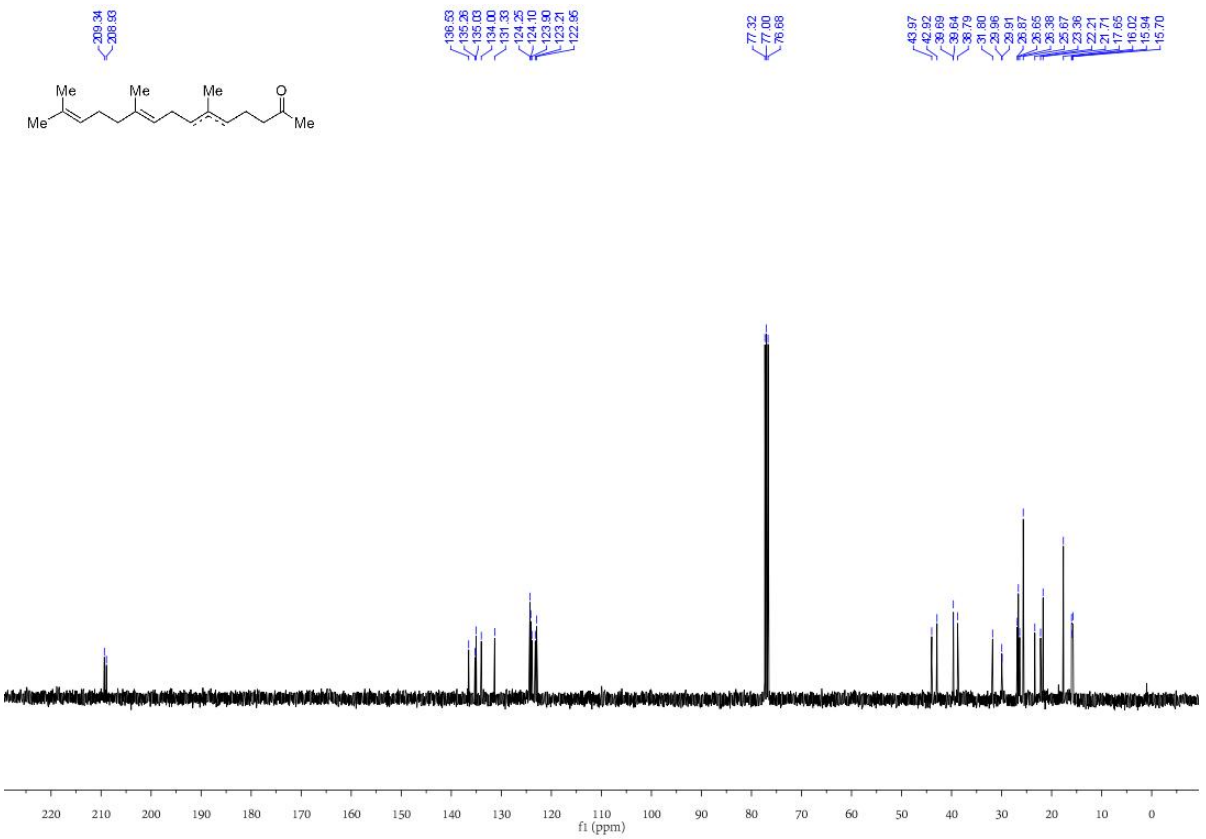

Figure S16. ^{13}C NMR spectrum of compound 1'.

Table S1. Summary of *Mac-bFS* positive mutations and the impact with respect to binding energy with farnesyl diphosphate (FPP).

Mutations	Productivity (fold)	Binding energy
wild	1.0000	-7.1
F11S	1.4625	-7.8
M35T	1.2324	-7.2
T319S	1.1186	-7.5
I434T	1.4036	-7.8
I460V	1.2066	-7.4

Table S2. Strains used in this study.

Strain	Genotype	Source
CEN.PK2-1D	*MATα, ura3–52, trp1–289, leu2-3,112, his3Δ1, MAL2–8C, SUC2*	EUROSCARF

	*CEN.PK2-1D ChrXII-2Δ::HygR*_P_{TEF1}_*Cas9, ChrXI-3Δ::*P_{GAL1}_*ERG8,* P_{GAL10}_*tHMG1,*	
JCR27	P_{GAL7}_*ERG12, ChrX-3Δ::*P_{GAL1}_*ERG13,* P_{GAL10}_*tHMG1, ChrXII-4Δ::*P_{GAL1}_*IDI1,* P_{GAL10}_*ERG10,* P_{GAL7}_*MVD1*	Ref.[7]
T16	*S. cerevisiae::* P_{GAL10}*-tHMG1;* P_{GAL10}*-FgJ03939;* P_{GAL1}*-ERG20*	Ref.[9]
F4	BL21(DE3)/pMH1/pFZ81/pFZ71	Ref.[10]
BFS1	JCR27 pBFS1	This work
BFS2	JCR27 pBFS2	This work
BFS4	JCR27 pBFS4	This work
BFS5	JCR27 pBFS5	This work
BFS6	JCR27 pBFS6	This work
BFS7	JCR27 pBFS7	This work
BFS45	JCR27 pBFS45	This work
JVA94	JCR27 *leu2Δ::*P_{GAL1}_*ERG20,*P_{GAL10}_*Mac-bFS, LEU2*	This work

JVA122	JCR27 *leu2Δ::*P_{GAL1}*_ERG20,* P_{GAL10}*_Mac-bFS(F11S,M35T,T319S,I434T,I460V), LEU2*	This work
JVA124	JCR27 *leu2Δ::*P_{GAL1}*_ERG20,* P_{GAL10}*_Mac-bFS(F11S,M35T,T319S,I434T,I460V), LEU2, ura3Δ::*P_{GAL1}*_Mac-bFS(F11S,M35T,T319S,I434T,I460V),* P_{GAL10}*_tHMG1, HIS3*	This work
JVA125	JCR27 *leu2Δ::*P_{GAL1}*_ERG20,* P_{GAL10}*_Mac-bFS(F11S,M35T,T319S,I434T,I460V), LEU2, ura3Δ::* P_{GAL1}*_Mac-bFS(F11S,M35T,T319S,I434T,I460V), HIS3*	This work
JVA127	JCR27 *leu2Δ::*P_{GAL1}*_ERG20,* P_{GAL10}*_Mac-bFS(F11S,M35T,T319S,I434T,I460V), LEU2, ura3Δ::*P_{GAL1}*_Mac-bFS(F11S,M35T,T319S,I434T,I460V),* P_{GAL10}*_tHMG1, HIS3, YPRCdelta15Δ::*P_{GAL1}*_Mac-bFS(F11S,M35T,T319S,I434T,I460V),* P_{GAL10}*_tHMG1, TRP1*	This work
JVA128	JCR27 *leu2Δ::*P_{GAL1}*_ERG20,* P_{GAL10}*_Mac-bFS(F11S,M35T,T319S,I434T,I460V), LEU2, ura3Δ::*P_{GAL1}*_Mac-bFS(F11S,M35T,T319S,I434T,I460V),* P_{GAL10}*_tHMG1, HIS3, YPRCdelta15Δ::*P_{GAL1}*_Mac-bFS(F11S,M35T,T319S,I434T,I460V), TRP1*	This work
JVA129	JCR27 *leu2Δ::*P_{GAL1}*_ERG20,* P_{GAL10}*_Mac-bFS(F11S,M35T,T319S,I434T,I460V), LEU2, ura3Δ::*P_{GAL1}*_Mac-bFS(F11S,M35T,T319S,I434T,I460V),*	This work

	P_{GAL10}*_Mac-bFS(F11S,M35T,T319S,I434T,I460V), HIS3*	
JVA134	JCR27 *leu2Δ::*P_{GAL1}*_ERG20,* P_{GAL10}*_Mac-bFS(F11S,M35T,T319S,I434T,I460V), LEU2, ura3Δ::*P_{GAL1}*_Mac-bFS(F11S,M35T,T319S,I434T,I460V),* P_{GAL10}*_Mac-bFS(F11S,M35T,T319S,I434T,I460V), HIS3, YPRCdelta15Δ::*P_{GAL1}*_Mac-bFS(F11S,M35T,T319S,I434T,I460V),* P_{GAL10}*_tHMG1, TRP1*	This work
JVA135	JCR27 *leu2Δ::*P_{GAL1}*_ERG20,* P_{GAL10}*_Mac-bFS(F11S,M35T,T319S,I434T,I460V), LEU2, ura3Δ::*P_{GAL1}*_Mac-bFS(F11S,M35T,T319S,I434T,I460V),* P_{GAL10}*_Mac-bFS(F11S,M35T,T319S,I434T,I460V), HIS3, YPRCdelta15Δ::* P_{GAL1}*_Mac-bFS(F11S,M35T,T319S,I434T,I460V),TRP1*	This work
JVA139	JCR27 *leu2Δ::*P_{GAL1}*_ERG20,* P_{GAL10}*_Mac-bFS(F11S,M35T,T319S,I434T,I460V), LEU2, ura3Δ::*P_{GAL1}*_Mac-bFS(F11S,M35T,T319S,I434T,I460V),* P_{GAL10}*_Mac-bFS(F11S,M35T,T319S,I434T,I460V), HIS3,*	This work

	YPRCdelta15Δ::P_{GAL1}*_Mac-bFS(F11S,M35T,T319S,I434T,I460V),* P_{GAL10}*_Mac-bFS(F11S,M35T,T319S,I434T,I460V),TRP1*	
JVA140	JCR27 *leu2Δ::*P_{GAL1}*_ERG20,* P_{GAL10}*_Mac-bFS(F11S,M35T,T319S,I434T,I460V), LEU2, ura3Δ::*P_{GAL1}*_Mac-bFS(F11S,M35T,T319S,I434T,I460V),* P_{GAL10}*_Mac-bFS(F11S,M35T,T319S,I434T,I460V), HIS3, YPRCdelta15Δ::*P_{GAL1}*_Mac-bFS(F11S,M35T,T319S,I434T,I460V),* P_{GAL10}*_Mac-bFS(F11S,M35T,T319S,I434T,I460V),TRP1, gal80Δ::URA3*	This work
JZL29	JCR27 *leu2Δ::*P_{GAL1}*_ERG20,* P_{GAL10}*_Mac-bFS(F11S,M35T,T319S,I434T,I460V), LEU2, ura3Δ::*P_{GAL1}*_Mac-bFS(F11S,M35T,T319S,I434T,I460V),* P_{GAL10}*_Mac-bFS(F11S,M35T,T319S,I434T,I460V), HIS3, YPRCdelta15Δ::*P_{GAL1}*_Mac-bFS(F11S,M35T,T319S,I434T,I460V),* P_{GAL10}*_Mac-bFS(F11S,M35T,T319S,I434T,I460V),TRP1, rDNAΔ::*P_{GAL1}*_PaCrtE,* P_{GAL10}*_BtCrtI, rDNAΔ::* P_{GAL1}*_PagCrtB,* P_{GAL10}*_tHMG1*	This work

JZL32	JCR27 *Leu2Δ::*P_{GAL1}*_ERG20,* P_{GAL10}*_Mac-bFS(F11S,M35T,T319S,I434T,I460V), LEU2, ura3Δ::*P_{GAL1}*_Mac-bFS(F11S,M35T,T319S,I434T,I460V),* P_{GAL10}*_Mac-bFS(F11S,M35T,T319S,I434T,I460V), HIS3, YPRCdelta15Δ::*P_{GAL1}*_Mac-bFS(F11S,M35T,T319S,I434T,I460V),* P_{GAL10}*_Mac-bFS(F11S,M35T,T319S,I434T,I460V),TRP1, rDNAΔ::*P_{GAL1}*_PaCrtE,* P_{GAL10}*_BtCrtI, rDNAΔ::*P_{GAL1}*_PagCrtB,* P_{GAL10}*_tHMG1, gal80Δ::URA3*	This work

Table S3. Plasmids used in this study.

Plasmids	Description	Source
pZY900	pRS426, *leu2Δ::LEU2*_P_{GAL1}*_ERG20,* P_{GAL10}*_LacZ, URA3*	This work
pBFS1	pRS426, *leu2Δ::LEU2*_P_{GAL1}*_ERG20,* P_{GAL10}*_Mac-bFS, URA3*	This work
pBFS2	pRS426, *leu2Δ::LEU2*_P_{GAL1}*_ERG20,* P_{GAL10}*_Hea-bFS, URA3*	This work
pBFS4	pRS426, *leu2Δ::LEU2*_P_{GAL1}*_ERG20,* P_{GAL10}*_Tac-bFS, URA3*	This work

pBFS5	pRS426, *leu2Δ::LEU2*_P_{GAL1}_*ERG20,* P_{GAL10}_*Cyc-bFS, URA3*	This work
pBFS6	pRS426, *leu2Δ::LEU2*_P_{GAL1}_*ERG20,* P_{GAL10}_*Las-bFS, URA3*	This work
pBFS7	pRS426, *leu2Δ::LEU2*_P_{GAL1}_*ERG20,* P_{GAL10}_*Aa-bFS, URA3*	This work
pBFS9	pRS426, *leu2Δ::LEU2*_P_{GAL1}_*ERG20,* P_{GAL10}_*Mac-bFS(F11S), URA3*	This work
pBFS12	pRS426, *leu2Δ::LEU2*_P_{GAL1}_*ERG20,* P_{GAL10}_*Mac-bFS(M35T), URA3*	This work
pBFS15	pRS426, *leu2Δ::LEU2*_P_{GAL1}_*ERG20,* P_{GAL10}_*Mac-bFS(T319S), URA3*	This work
pBFS18	pRS426, *leu2Δ::LEU2*_P_{GAL1}_*ERG20,* P_{GAL10}_*Mac-bFS(I434T), URA3*	This work
pBFS20	pRS426, *leu2Δ::LEU2*_P_{GAL1}_*ERG20,* P_{GAL10}_*Mac-bFS(I460V), URA3*	This work
pBFS45	pRS426, *leu2Δ::LEU2*_P_{GAL1}_*ERG20,* P_{GAL10}_*Mac-bFS(F11S,M35T,T319S,I434T,I460V), URA3*	This work
pBFS45-P2	pRS426, *ura3Δ::*P_{GAL1}_*Mac-bFS(F11S,M35T,T319S,I434T,I460V),* P_{GAL10}_*tHMG1, HIS3*	This work
pBFS45-P3	pRS426, *ura3Δ::*P_{GAL1}_*Mac-bFS(F11S,M35T,T319S,I434T,I460V), HIS3*	This work
pBFS45-P4	pRS426, *ura3Δ::*P_{GAL1}_*Mac-bFS(F11S,M35T,T319S,I434T,I460V),* P_{GAL10}_*Mac-bFS(F11S,M35T,T319S,I434T,I460V), HIS3*	This work

pBFS45-P5	pRS426, *YPRCdelta15Δ::*P_{GAL1}*_Mac-bFS(F11S,M35T,T319S,I434T,I460V),* P_{GAL10}*_tHMG1, TRP1*	This work
pBFS45-P6	pRS426, *YPRCdelta15Δ::*P_{GAL1}*_Mac-bFS(F11S,M35T,T319S,I434T,I460V), TRP1*	This work
pBFS45-P7	pRS426, *YPRCdelta15Δ::*P_{GAL1}*_Mac-bFS(F11S,M35T,T319S,I434T,I460V),* P_{GAL10}*_Mac-bFS(F11S,M35T,T319S,I434T,I460V), TRP1*	This work
pXZ162	pCas derived,[11] P_{TEF1}*_iCas9,* P_{SNR52}_gRNA.rDNA	This work
pXZ147	pRS426, *rDNAΔ::*P_{GAL1}*_PaCrtE,* P_{GAL10}*_BtCrtI*	This work
pXZ148	pRS426, *rDNAΔ::*P_{GAL1}*_PagCrtB,* P_{GAL10}*_tHMG1*	This work

Table S4. Primers used in this study.

Plasmids	Fragments	Template	Primer	Sequence（5’-3’）
pZY900	Leu2 left arm	S288C	900-1F	ACTAAAGGGAACAAAAGCTGGAGCTCTAGTAGTTTAAACATAACGAGAACACACAGGGG
			900-1R	CATTAAAGTAACTTAAGGAGTTAAATTTAAGCAAGGATTTTCTTAACTT

			CTTC
T_{TDH2}	S288C	900-2F	GAAGTTAAGAAAATCCTTGCTTAAATTTAACTCCTTAAGTTACTTTAATG ATTTAG
		900-2R	TCGAAGGCTTTAATTTGCGCGAAAAGCCAATTAGTGTGATA
T_{CYC1}	CEN.PK 2-1D	900-3F	TAGTATCACACTAATTGGCTTTTCGCGCAAATTAAAGCCTTCGAGC
		900-3R	GGGACGCGCCCTGTAGCGGCTGAGGTCTCAACAGGCCCCTTTTCCTT TG
lacZ	pCas	900-4F	CATGATATCGACAAAGGAAAAGGGGCCTGTTGAGACCTCAGCCGCTA CAGGGCGC
		900-4R	gaatttttgaaaattcaatataaATGTGAGACCACCATGATTACGCCAAGCG
P_{GAL10}-P_{GAL1}	CEN.PK 2-1D	900-5F	TAATCATGGTGGTCTCACATttatattgaattttcaaaaattcttactttttttttg

		900-5R	ATCTCTCTCTCCTAATTTCTTTTTCTGAAGCcattatagttttttctccttgacgttaaagt
ERG20-T_{ERG20}	S288C	900-6F	ttaacgtcaaggagaaaaaactataatgGCTTCAGAAAAAGAAATTAGGA
		900-6R	ATGTACAAATATCATAAAAAAAGAGAATCTTTTTAAAAAAAATCCTTGGACTAGTCACG
Leu2 right arm	S288C	900-7F	ACTAGTCCAAGGATTTTTTTTAAAAAGATTCTCTTTTTTTATGATATTTGTACATAAAC
		900-7R	GCGCCATTCGCCATTCAGGCTGCGCAACTGTTGTTTAAACGACAACGACCAAGCTCACA
URA3 marker, AmpR, ori	pRS426	900-8F	GATGTGAGCTTGGTCGTTGTCGTTTAAACAACAGTTGCGCAGCCTGAATG
		900-8R	TCAACAGTATAGAACCGTGGATGATGTGGT**t**TCTACAGGATCTGACATTATTATTGTTG
URA3 marker,	pRS426	900-9F	ATAGTCCTCTTCCAACAATAATAATGTCAGATCCTGTAGA**a**ACCACATC

	AmpR, ori			ATCCACGGTT
			900-9R	AGGGCTTACCATCTGGCCCCAGTGCTGCAATGATACCGCG**c**GACCCA CGCTCACCGGCT
	URA3 marker, AmpR, ori	pRS426	900-10F	TGATAAATCTGGAGCCGGTGAGCGTGGGTC**g**CGCGGTATCATTGCAG CACTGGGGCCAG
			900-10R	CGATAGCGCCCCTGTGTGTTCTCGTTATGTTTAAACTACTAGAGCTCC AGCTTTTGTTC
pBFS1	*Mac-bFS*	Mac-bFS	pBFS1-1 F	AAAGGTCTCACTGTTCAAATGACCATTGGGTGGACAAAG
			pBFS1-1 R	AAAGGTCTCAaATGTCTACTATCCCTGTTTCCAGTG
pBFS2	*Hea-bFS*	Hea-bFS	pBFS2-1 F	aaaggtctcaCTGTTCAGATAACAGCTGGTTGAACGA

			pBFS2-1 R	AAAGGTCTCAaATGGTCTGTATTTCCGACTTTTTC
pBFS4	*Tac-bFS*	Tac-bFS	pBFS4-1 F	aaaggtctcaCTGTTCAGACAATCATTGGTTGAACAA
			pBFS4-1 R	AAAGGTCTCAaATGTTGAGAAAGATTTCTTGTCCTAG
pBFS5	*Cyc-bFS*	Cyc-bFS	pBFS5-1 F	aaaggtctcaCTGTTCAAATCAATGGGTGAACTAGC
			pBFS5-1 R	AAAGGTCTCAaATGTCCTCCTTTGAAATGTCCA
pBFS6	*Las-bFS*	Las-bFS	pBFS6-1 F	aaaggtctcaCTGTTCAAACGGACATGGAGTTGG
			pBFS6-1	AAAGGTCTCAaATGTCTTCTCCAGTTTTGTGCTC

			R	
pBFS7	*Aa-bFS*	Aa-bFS	pBFS7-1 F	AAAGGTCTCACTGTTCAAACAACCATTGGATGAACAAAGAAAGAC
			pBFS7-1 R	AAAGGTCTCaaATGTCTACTTTGCCAATCTCTTCAGTTTC
For pBFS1 mutant library screening	Mac-bFS variants	pBFS1	pBFS1-mutation-F	ATTACATGATATCGACAAAGGAAAAGGGGCCTGTTCAAATGACCATTG GGTGGACAAAG
			pBFS1-mutation-R	aaaaaaagtaagaatttttgaaaattcaatataaATGTCTACTATCCCTGTTTCCAGTG
pBFS45	*Mac-bFS-I460V*	pBFS20	pBFS1-1	AAAGGTCTCACTGTTCAAATGACCATTGGGTGGACAAAG

		F	
		pBFS45-2R	TTCTTCTTACCCACCAATCGTCAAGGCTTCCTGTGTTATTG
Mac-bFS-I434T	pBFS18	pBFS45-3F	ACACAGGAAGCCTTGACGATTGGTGGGTAAGAAGAAAC
		pBFS45-3R	ACTTACGGTTTGATGACTGCTAGATCCTACGTTGGTAG
Mac-bFS-T319S	pBFS15	pBFS45-4F	ACCAACGTAGGATCTAGCAGTCATCAAACCGTAAGTACCG
		pBFS45-4R	AGAATGTTCTTGATGAAGTCTTGTATGTGGCTTGTTGTTTTG
Mac-bFS-M35T	pBFS12	pBFS45-5F	AAGCCACATACAAGACTTCATCAAGAACATTCTGGTTC

			pBFS45-5R	TGTTGTCAGACACACCACCAACTTTTCTGCTTCTATCTGG
	Mac-bFS-F11S	pBFS9	pBFS45-6F	GAAGCAGAAAAGTTGGTGGTGTGTCTGACAACATC
			pBFS45-6R	AAAGGTCTCaaATGTCTACTATCCCTGTTTCCAGTGTTTCTTCCTCTAG TTCTGCCTC
pBFS45-P2	Ura3 left arm	CEN.PK 2-1D	pAFS1-P2-1F	ATTAACCCTCACTAAAGGGAACAAAAGCGTTTAAACacgcagataattccaggt atttt
			pAFS1-P2-1R	AATACGACTCACTATAGGGCGAATTGGGTACcttcgtttcctgcaggtttttgt
	HIS3 marker	pRS423	pAFS1-P2-2F	caaaaacctgcaggaaacgaagGTACCCAATTCGCCCTATAGTGAG
			pAFS1-P	GTTTTGGGACGCTCGAAGGCTTTAATTTGCTCACAGCTTGTCTGTAAG

		2-2R	CG
T_{CYC1}	CEN.PK 2-1D	pAFS1-P 2-3F	TTGTCTGCTCCCGGCATCCGCTTACAGACAAGCTGTGAGCAAATTAAA GCCTTCGAGCG
		pAFS1-P 2-3R	GTTTGAAAGATGGGTCCGTCACCTGCATTAAATCCTAAACAGGCCCCT TTTCCTTTGTC
tHMG1	S288C	pAFS1-P 2-4F	TAATTACATGATATCGACAAAGGAAAAGGGGCCTGTTTAGGATTTAAT GCAGGTGACGG
		pAFS1-P 2-4R	gaatttttgaaaattcaatataaATGGTTTTAACCAATAAAACAGTCAT
P_{GAL10}-P_{GAL1}	CEN.PK 2-1D	pAFS1-P 2-5F	GTTTTATTGGTTAAAACCATttatattgaattttcaaaaattcttacttttttttgg
		pBFS45-P2-5R	CTGGAAACAGGGATAGTAGACATtatagtttttctccttgacgttaaagt

Mac-bFS(F11S, M35T,T319S,I434T,I460V)	pBFS45	pBFS45-P2-6F	ctatactttaacgtcaaggagaaaaaactataATGTCTACTATCCCTGTTTCC
		pBFS45-P2-6R	GAAAAAAATTGATCTATCGATTTCAATTCAATTCAATTCAAATGACCATTGGGTGGAC
T_{PGK1}	CEN.PK2-1D	pBFS45-P2-7F	GTCCACCCAATGGTCATTTGAATTGAATTGAATTGAAATCGATAGATCAAT
		pAFS1-P2-7R	ttgaagctctaatttgtgagtttagtatacatgcatttacAACGAACGCAGAATTTTCG
Ura3 right arm	CEN.PK2-1D	pAFS1-P2-8F	GTTTAATAACTCGAAAATTCTGCGTTCGTTgtaaatgcatgtatactaaactcacaaat
		pAFS1-P2-8R	GACGGTCACAGCTTGTCTGTGTTTAAACcgtttaagggcaaatgtactct

	URA3 marker, AmpR, ori	pRS426	pAFS1-P 2-9F	agagtacatttgcccttaaacgGTTTAAACACAGACAAGCTGTGACCGTC
			pAFS1-P 2-9R	tgcttcaaaatacctggaattatctgcgtGTTTAAACGCTTTTGTTCCCTTTAGTGAGG
pBFS45-P3	Ura3 left arm	CEN.PK 2-1D	pAFS1-P 2-1F	ATTAACCCTCACTAAAGGGAACAAAAGCGTTTAAACacgcagataattccaggtatttt
			pAFS1-P 2-1R	AATACGACTCACTATAGGGCGAATTGGGTACcttcgtttcctgcaggtttttgt
	HIS3 marker	pRS423	pAFS1-P 2-2F	caaaaacctgcaggaaacgaagGTACCCAATTCGCCCTATAGTGAG
			pAFS1-P 2-2R	GTTTTGGGACGCTCGAAGGCTTTAATTTGCTCACAGCTTGTCTGTAAGCG
	T_{CYC1}	CEN.PK	pAFS1-P	TTGTCTGCTCCCGGCATCCGCTTACAGACAAGCTGTGAGCAAATTAAA

	2-1D	2-3F	GCCTTCGAGCG
		pAFS1-P 3-3R	gaatttttgaaaattcaatataaACAGGCCCCTTTTCCTTTGTC
P_{GAL10}-P_{GAL1}	CEN.PK 2-1D	pAFS1-P 3-5F	GACAAAGGAAAAGGGGCCTGTttatattgaattttcaaaaattc
		pBFS45-P3-5R	GGAAACAGGGATAGTAGACATtatagttttttctccttgacg
Mac-bFS(F11S, M35T,T319S,I434T,I460V)	pBFS45	pBFS45-P3-6F	cgtcaaggagaaaaaactataATGTCTACTATCCCTGTTTCC
		pBFS45-P3-6R	CGATTTCAATTCAATTCAATTCAAATGACCATTGGGTGGAC
T_{PGK1}	CEN.PK	pBFS45-	GTCCACCCAATGGTCATTTGAATTGAATTGAATTGAAATCG

		2-1D	P3-7F	
			pAFS1-P2-7R	ttgaagctctaatttgtgagtttagtatacatgcatttacAACGAACGCAGAATTTTCG
	Ura3 right arm	CEN.PK 2-1D	pAFS1-P2-8F	GTTTAATAACTCGAAAATTCTGCGTTCGTTgtaaatgcatgtatactaaactcacaat
			pAFS1-P2-8R	GACGGTCACAGCTTGTCTGTGTTTAAACcgtttaagggcaaatgtactct
	URA3 marker, AmpR, ori	pRS426	pAFS1-P2-9F	agagtacatttgcccttaaacgGTTTAAACACAGACAAGCTGTGACCGTC
			pAFS1-P2-9R	tgcttcaaaatacctggaattatctgcgtGTTTAAACGCTTTTGTTCCCTTTAGTGAGG
pBFS45-P4	Ura3 left arm	CEN.PK 2-1D	pAFS1-P2-1F	ATTAACCCTCACTAAAGGGAACAAAAGCGTTTAAACacgcagataattccaggtatttt

		pAFS1-P2-1R	AATACGACTCACTATAGGGCGAATTGGGTACcttcgtttcctgcaggtttttgt
HIS3 marker	pRS423	pAFS1-P2-2F	caaaaacctgcaggaaacgaagGTACCCAATTCGCCCTATAGTGAG
		pAFS1-P2-2R	GTTTTGGGACGCTCGAAGGCTTTAATTTGCTCACAGCTTGTCTGTAAGCG
T_{CYC1}	CEN.PK2-1D	pAFS1-P2-3F	TTGTCTGCTCCCGGCATCCGCTTACAGACAAGCTGTGAGCAAATTAAAGCCTTCGAGCG
		pBFS45-P4-3R	GTCCACCCAATGGTCATTTGAACAGGCCCCTTTTCCTTTGTC
Mac-bFS(F11S, M35T,T319S,I434T,I460V)	pBFS45	pBFS45-P4-4F	TAATTACATGATATCGACAAAGGAAAAGGGGCCTGTTCAAATGACCATTGGGTGGAC

		pBFS45-P4-4R	gaatttttgaaaattcaatataaATGTCTACTATCCCTGTTTCCA
P_{GAL10}-P_{GAL1}	CEN.PK 2-1D	pBFS45-P4-5F	CAGGGATAGTAGACATttatattgaattttcaaaaattcttacttttttttg
		pBFS45-P4-5R	GGAAACAGGGATAGTAGACATtatagtttttctccttgacgttaaagt
Mac-bFS(F11S, M35T,T319S,I434T,I460V)	pBFS45	pBFS45-P4-6F	ctctatactttaacgtcaaggagaaaaaactataATGTCTACTATCCCTGTTTCC
		pBFS45-P4-6R	AAATTGATCTATCGATTTCAATTCAATTCAATTCAAATGACCATTGGGTGGAC
T_{PGK1}	CEN.PK 2-1D	pBFS45-P4-7F	CCACCCAATGGTCATTTGAATTGAATTGAATTGAAATCGATAGATCAAT

			pAFS1-P2-7R	ttgaagctctaatttgtgagtttagtatacatgcatttacAACGAACGCAGAATTTTCG
	Ura3 right arm	CEN.PK2-1D	pAFS1-P2-8F	GTTTAATAACTCGAAAATTCTGCGTTCGTTgtaaatgcatgtatactaaactcacaaat
			pAFS1-P2-8R	GACGGTCACAGCTTGTCTGTGTTTAAACcgtttaagggcaaatgtactct
	URA3 marker, AmpR, ori	pRS426	pAFS1-P2-9F	agagtacatttgcccttaaacgGTTTAAACACAGACAAGCTGTGACCGTC
			pAFS1-P2-9R	tgcttcaaaatacctggaattatctgcgtGTTTAAACGCTTTTGTTCCCTTTAGTGAGG
pBFS45-P5	YPRCdelta15 left arm	CEN.PK2-1D	pAFS1-P5-1F	CTAAAGGGAACAAAAGCGCGGCCGCGGCAATTTGGTACAAAAATCACG
			pAFS1-P	CTATATTATATATATAGTAATGTCGTTTTTGCGAAACCCTATGCTC

		5-1R	
TRP1 marker	pRS424	pAFS1-P 5-2F	GAGCATAGGGTTTCGCAAAAACGACATTACTATATATATAATATAG
		pAFS1-P 5-2R	GCTCGAAGGCTTTAATTTGCCCTGATGCGGTATTTTCTCC
T_{CYC1}	CEN.PK 2-1D	pAFS1-P 5-3F	GGAGAAAATACCGCATCAGGGCAAATTAAAGCCTTCGAGCG
		pAFS1-P	GTTTGAAAGATGGGTCCGTCACCTGCATTAAATCCTAAACAGGCCCCT
		7-3R	TTTCCTTTGTC
tHMG1	S288C	pAFS1-P	TAATTACATGATATCGACAAAGGAAAAGGGGCCTGTTTAGGATTTAAT
		7-4F	GCAGGTGACGG
		pAFS1-P 7-4R	gaatttttgaaaattcaatataaATGGTTTTAACCAATAAAACAGTCATTT

P_{GAL10}-P_{GAL1}	CEN.PK 2-1D	pAFS1-P 7-5F	GTTTTATTGGTTAAAACCATttatattgaattttcaaaaattcttacttttttttg
		pBFS45-P5-5R	GGAAACAGGGATAGTAGACATtatagttttttctccttgacg
Mac-bFS(F11S, M35T,T319S,I434T,I460V)	pBFS45	pBFS45-P5-6F	cgtcaaggagaaaaaactataATGTCTACTATCCCTGTTTCC
		pBFS45-P5-6R	CGATTTCAATTCAATTCAATTCAAATGACCATTGGGTGGAC
T_{PGK1}	CEN.PK 2-1D	pBFS45-P5-7F	GTCCACCCAATGGTCATTTGAATTGAATTGAATTGAAATCG
		pAFS1-P 5-7R	GCTCATCCCGACCTTCCATTAACGAACGCAGAATTTTCGAG

	YPRCdelta15 right arm	CEN.PK 2-1D	pAFS1-P 5-8F	CTCGAAAATTCTGCGTTCGTTAATGGAAGGTCGGGATGAGC
			pAFS1-P 5-8R	AGACGGTCACAGCTTGTCTGTGCGGCCGCGCTTCTAATAAACCGATG AACGC
	AmpR, ori	pRS426	pAFS1-P 5-9F	GCGTTCATCGGTTTATTAGAAGCGCGGCCGCACAGACAAGCTGTGAC CGTCT
			pAFS1-P 5-9R	TTTTGTACCAAATTGCCGCGGCCGCGCTTTTGTTCCCTTTAGTGAGG
pBFS45-P6	YPRCdelta15 left arm	CEN.PK 2-1D	pAFS1-P 5-1F	CTAAAGGGAACAAAAGCGCGGCCGCGGCAATTTGGTACAAAAATCAC G
			pAFS1-P 5-1R	CTATATTATATATATAGTAATGTCGTTTTTGCGAAACCCTATGCTC
	TRP1 marker	pRS424	pAFS1-P	GAGCATAGGGTTTCGCAAAAACGACATTACTATATATATAATATAG

		5-2F	
		pAFS1-P 6-2R	GCTGAATGGGCAGTTCGAATACCTGATGCGGTATTTTCTCC
T_{GPM1}	S288C	pAFS1-P 6-3F	GGAGAAAATACCGCATCAGGTATTCGAACTGCCCATTCAGC
		pAFS1-P 6-3R	gtaagaatttttgaaaattcaatataaGTCTGAAGAATGAATGATTTGATGAT
P_{GAL10}-P_{GAL1}	CEN.PK 2-1D	pAFS1-P 6-5F	AATCATTCATTCTTCAGACttatattgaattttcaaaaattcttacttttttttg
		pBFS45-P6-5R	GGAAACAGGGATAGTAGACATtatagtttttctccttgacg
Mac-bFS(F11S, M35T,T319S,I4	pBFS45	pBFS45-P6-6F	cgtcaaggagaaaaaactataATGTCTACTATCCCTGTTTCC

34T,I460V)

		pBFS45-P6-6R	CGATTTCAATTCAATTCAATTCAAATGACCATTGGGTGGAC
T_{PGK1}	CEN.PK 2-1D	pBFS45-P6-7F	GTCCACCCAATGGTCATTTGAATTGAATTGAATTGAAATCG
		pAFS1-P5-7R	GCTCATCCCGACCTTCCATTAACGAACGCAGAATTTTCGAG
YPRCdelta15 right arm	CEN.PK 2-1D	pAFS1-P5-8F	CTCGAAAATTCTGCGTTCGTTAATGGAAGGTCGGGATGAGC
		pAFS1-P5-8R	AGACGGTCACAGCTTGTCTGTGCGGCCGCGCTTCTAATAAACCGATGAACGC
AmpR, ori	pRS426	pAFS1-P5-9F	GCGTTCATCGGTTTATTAGAAGCGCGGCCGCACAGACAAGCTGTGACCGTCT

			pAFS1-P5-9R	TTTTGTACCAAATTGCCGCGGCCGCGCTTTTGTTCCCTTTAGTGAGG
pBFS45-P7	YPRCdelta15 left arm	CEN.PK 2-1D	pAFS1-P5-1F	CTAAAGGGAACAAAAGCGCGGCCGCGGCAATTTGGTACAAAAATCACG
			pAFS1-P5-1R	CTATATTATATATATAGTAATGTCGTTTTTGCGAAACCCTATGCTC
	TRP1 marker	pRS424	pAFS1-P5-2F	GAGCATAGGGTTTCGCAAAAACGACATTACTATATATATAATATAG
			pAFS1-P5-2R	GCTCGAAGGCTTTAATTTGCCCTGATGCGGTATTTTCTCC
	T_{CYC1}	CEN.PK 2-1D	pAFS1-P5-3F	GGAGAAAATACCGCATCAGGGCAAATTAAAGCCTTCGAGCG
			pBFS45-	CTTTGTCCACCCAATGGTCATTTGAACAGGCCCCTTTTCCTTTGTC

		P7-3R	
Mac-bFS(F11S, M35T,T319S,I434T,I460V)	pBFS45	pBFS45-P7-4F	ATCGACAAAGGAAAAGGGGCCTGTTCAAATGACCATTGGGTGGAC
		pBFS45-P7-4R	gtaagaatttttgaaaattcaatataaATGTCTACTATCCCTGTTTCCAGT
P_{GAL10}-P_{GAL1}	CEN.PK 2-1D	pBFS45-P7-5F	CAGGGATAGTAGACATttatattgaattttcaaaaattcttacttttttttg
		pBFS45-P7-5R	CACTGGAAACAGGGATAGTAGACATtatagtttttctccttgacgttaaagt
Mac-bFS(F11S, M35T,T319S,I434T,I460V)	pBFS45	pBFS45-P7-6F	cgtcaaggagaaaaaactataATGTCTACTATCCCTGTTTCCAGTG

		pBFS45-P7-6R	GATCTATCGATTTCAATTCAATTCAATTCAAATGACCATTGGGTGGAC
T_{PGK1}	CEN.PK 2-1D	pBFS45-P7-7F	CCACCCAATGGTCATTTGAATTGAATTGAATTGAAATCGATAGATCAAT
		pAFS1-P5-7R	GCTCATCCCGACCTTCCATTAACGAACGCAGAATTTTCGAG
YPRCdelta15 right arm	CEN.PK 2-1D	pAFS1-P5-8F	CTCGAAAATTCTGCGTTCGTTAATGGAAGGTCGGGATGAGC
		pAFS1-P5-8R	AGACGGTCACAGCTTGTCTGTGCGGCCGCGCTTCTAATAAACCGATG AACGC
AmpR, ori	pRS426	pAFS1-P5-9F	GCGTTCATCGGTTTATTAGAAGCGCGGCCGCACAGACAAGCTGTGAC CGTCT
		pAFS1-P	TTTTGTACCAAATTGCCGCGGCCGCGCTTTTGTTCCCTTTAGTGAGG

			5-9R	
pXZ162	P_{SNR52}_gRNA.r DNA, *KlURA3*	pKlURA3 100	1621-F	AAAGGTCTCAgatc**TCCAAAGTGACAGGTGCCCC**GTTTTAGAGCTAGAA ATAGCAAGTT
			1621-R	aaaggtctcaaaacTCTAGACTTTTTCGATGATGTAGTTTC
	pCas			
pXZ147	rDNA left arm	S288C	1471-F	GCTCGGTACCCGGGGATCCTCTAGAGATtGTTTAAACTTTCCTCTAATC AGGTTCCACC
			1471-R	GGTTTTGGGACGCTCGAAGGCTTTAATTTGCTCACTTTGGAAAAAAAA TATACGCTAAG
	P_{GAL10}-*BtCrtI*-$T_{C\ YC1}$	pZY184[1]	1472-F	TCTCCAAAAATCTTAGCGTATATTTTTTTTCCAAAGTGAGCAAATTAAA GCCTTCGAGC
			1114-F	ttcctcttcataaccataaaagctag
	P_{GAL1}-*PaCrtE*-T	pZY153[1]	1115-R	actgctccgaacaataaagat

	GPM1			
			1473-R	TAAAAAATAGTGAGGAACTGGGTTACCCGGGGCACCTGTATTCGAACT GCCCATTCAGC
	rDNA right arm	S288C	1474-F	CACCAATTGCAAAGGGAAAAGCTGAATGGGCAGTTCGAATACAGGTG CCCCGGGTAACC
			1474-R	CCAAGCTTGCATGCCTGCAGGTCGACGATGTTTAAACCATGAGAGTA GCAAACGTAAGT
	pMD19T			
pXZ148	rDNA left arm	S288C	1471-F	GCTCGGTACCCGGGGATCCTCTAGAGATtGTTTAAACTTTCCTCTAATC AGGTTCCACC
			1481-R	ATAAAAAATGTTTATCCATTGGACCGTGTATCACTTTGGAAAAAAAATA TACGCTAAGA
	P_{GAL10}-*tHMG1*-	pZY141[1]	1482-F	CCAAAAATCTTAGCGTATATTTTTTTTCCAAAGTGATACACGGTCCAAT

T_{ACT1}			GGATAAACAT
		1114-F	ttcctcttcataaccataaaagctag
P_{GAL1}-*PagCrtB*-T_{PGK1}	pZY184	1115-R	actgctccgaacaataaagat
		1483-R	GTAAAAAATAGTGAGGAACTGGGTTACCCGGGGCACCTGAACGAACG CAGAATTTTCGA
rDNA right arm	S288C	1484-F	GCGTATTTTAAGTTTAATAACTCGAAAATTCTGCGTTCGTTCAGGTGCC CCGGGTAACC
		1474-R	CCAAGCTTGCATGCCTGCAGGTCGACGATGTTTAAACCATGAGAGTA GCAAACGTAAGT
pMD19T			

Supplemental References

1. Shi, B., Ma, T., Ye, Z., et al. (2019). Systematic metabolic engineering of *Saccharomyces cerevisiae* for lycopene overproduction. J. Agric. Food Chem. ***67***, 11148-11157.

2. Engler, C., Kandzia, R., and Marillonnet, S. (2008). A one pot, one step, precision cloning method with high throughput capability. PloS one ***3***, e3647.

3. Gibson, D.G. (2011). Enzymatic assembly of overlapping DNA fragments. Methods Enzymol. ***498***, 349-361.

4. Gibson, D.G., Benders, G.A., Axelrod, K.C., et al. (2008). One-step assembly in yeast of 25 overlapping DNA fragments to form a complete synthetic *Mycoplasma genitalium* genome. Proc. Natl. Acad. Sci. U. S. A. ***105***, 20404-20409.

5. Gietz, R.D., and Schiestl, R.H. (2007). High-efficiency yeast transformation using the LiAc/SS carrier DNA/PEG method. Nat. Protoc. ***2***, 31-34.

6. Paddon, C.J., Westfall, P.J., Pitera, D.J., et al. (2013). High-level semi-synthetic production of the potent antimalarial artemisinin. Nature ***496***, 528-532.

7. Siemon, T., Wang, Z., Bian, G., et al. (2020). Semisynthesis of plant-derived englerin A enabled by microbe engineering of guaia-6,10(14)-diene as building block. J. Am. Chem. Soc. ***142***, 2760-2765.

8. Van Hoek, P., de Hulster, E., van Dijken, J.P., and Pronk, J.T. (2000). Fermentative capacity in high-cell-density fed-batch cultures of baker's yeast. Biotechnol. Bioeng. ***68***, 517-523.

9. Bian, G., Hou, A., Yuan, Y., et al. (2018). Metabolic engineering-based rapid characterization of a sesquiterpene cyclase and the skeletons of fusariumdiene and fusagramineol from *Fusarium graminearum*. Org. Lett. ***20***, 1626-1629.

10. Zhu, F., Zhong, X., Hu, M., et al. (2014). In vitro reconstitution of mevalonate pathway and targeted engineering of farnesene overproduction in *Escherichia coli*. Biotechnol. Bioeng. ***111***, 1396-1405.

11. Zhang, Y., Wang, J., Wang, Z., et al. (2019). A gRNA-tRNA array for CRISPR-Cas9 based rapid multiplexed genome editing in *Saccharomyces cerevisiae*. Nat. Commun. ***10***, 1053.